Doctoral dissertation

# The Importance of Renalase Gene in Exercise-Enhanced Glucose Tolerance via The Diversity of Microbiota

2022

Doctoral Program in Sports Medicine,

Graduate School of Comprehensive Human Sciences,

University of Tsukuba

Fang Hui

# Table of contents

This doctoral dissertation is based on the following sub-thesis.

Study 1 and 2

1. Hui Fang, Kai Aoki, Katsuyuki Tokinoya, Takehito Sugasawa, Masato Yonamine, Yasushi Kawakami and Kazuhiro Takekoshi, Effects of High-Fat Diet on the Gut Microbiota of Renalase Gene Knockout Mice. Obesities, 2022. 2(3): p. 303-316.

Study 3

2. Hui Fang, Kai Aoki, Katsuyuki Tokinoya, Yasuko Yoshida, Masato Yonamine, Yasushi Kawakami and Kazuhiro Takekoshi, Fecal supernatant from renalase gene knockout mice weakens the AKT/JNK pathway to decrease the expression of Pc1/3 and Boc-Arg-Val-Arg-Arg-MCA cleaving activity in STC-1 cell line. International Journal of Analytical Bio-Science. Accepted, Nov.18 2022.

# List of Tables

# List of Figures

# Abbreviations

| | |
|---|---|
| *Rnls* | renalase gene |
| T2D | type 2 diabetes |
| GM | gut microbiota |
| BG | blood glucose |
| PI3K-AKT | phosphatidylinositol 3-kinase/ Protein Kinase B |
| IPGTT | intraperitoneal glucose tolerance test |
| TG | triglycerides |
| BW | body weight |
| IPITT | intraperitoneal insulin tolerance test |
| JNK | jun amino terminal kinase |
| Pc1/3 | prohormone converting enzyme 1/3 |
| HDL-C | high density lipoprotein-cholesterol |
| MAPK | mitogen-activated protein kinase |
| VDL-C | low density lipoprotein-cholesterol |
| TC | total cholesterol |
| TP | total protein |
| AMPK | AMP-activated protein kinase |

# I. Introduction

Hyperglycemia is the typical character for diabetes [1]. Furthermore, it is the main reason to result in many complications, such as heart attacks, strokes, kidney failure, and blindness [2-4]. The causes of hyperglycemia and damages are showed in Figure 1 and 2. Nowadays, diabetes has been become the one another killer for human health after cancers. According to the World Health Organization, it directly caused 1.5 million deaths in 2019. Notably, the incidence of diabetes has shown a trend towards younger people in recent years [5, 6]. the number of adults with diabetes will reach 783 million by 2045 according to the report from International Diabetes Federation. Among them, over 95% diabetes belong to type 2 diabetes (T2D) [7]. As we all known, number of factors including genetics, obesity, and physical inactivity trigger T2D [8, 9]. The complexity of its pathogenesis and the prevalence of its existence determine the difficulty of diagnose and treatment. Hence, continuing to dig the underling mechanism of hyperglycemia, regulating blood glucose (BG) more effectively and rationally to is still the facing challenge to decrease the incidence of T2D and its complications.

According to the latest guidance statement from American College of Sports Medicine and American Diabetes Association, T2D are recommended to do exercise (Figure 3). Regular aerobic exercise training (e.g. jogging, swimming) can increase insulin sensitivity, improve BG in adults with T2D, reduce the time of hyperglycemia; resistance training (e.g. push-ups, resistance bands) improves glucose metabolism in elderly patients with T2D [10]. Of course, diet therapy is also another environmental factor for alleviating T2D. Recent studies showed that a high-fiber diet can alleviate body weight and BG, thereby reducing the risk of T2D and its complications [11, 12]. Hence, in clinical treatment, exercise therapy, together with diet therapy and drug therapy is also known as the "troika" for the treatment of T2D.

Gut microbiota (GM) is closely related to T2D was reported recently [13-15]. Unhealthy lifestyle will destroy the balance of GM. Some studies showed that the percentage of *Lactobacillus*, *Bifidobacterium*, *Akkermansia* is reduced in the gut of T2D, while a high-fiber diet or probiotics can elevate the abundance of *Lactobacillus*,

*Bifidobacterium*, and improve glucose metabolism [16-18]. Some latest studies showed that low intensity exercise and moderate intensity exercise are contributed to GM homeostasis (Figure 4) [19-21]. Notably, GM is susceptible to the combined influence of the environment and host genes so that exhibited the adaptations to host metabolism [22]. In other words, it is not only environment factors but also host gene also able to shift GM, thereby, lead to abnormalities in the host metabolism.

Renalase was found in the kidney as a FAD-dependent amine oxidase reported in 2005 [23]. Subsequently identified that other tissues, such as muscle, intestine, heart, liver also expresses renalase. It suggested that renalase is somehow involved in maintaining homeostasis of the host. Some studies have shown that renalase level of blood and tissues has close relationship with metabolic disease and several cancers [24-26]. The single nucleotide polymorphism of renalase gene *(Rnls)* can accelerate the progression of T2D and its complications [27]. Representative summary is showed in Figure 5. However, the regulatory mechanism of *Rnls* involves in the progression of T2D, and even its' role involved in exercise therapy on alleviating T2D are ambiguous.

Therefore, to reveal the importance of *Rnls* in exercise-enhanced glucose tolerance through the diversity of gut microbiota is identified as the purpose of my doctoral thesis.

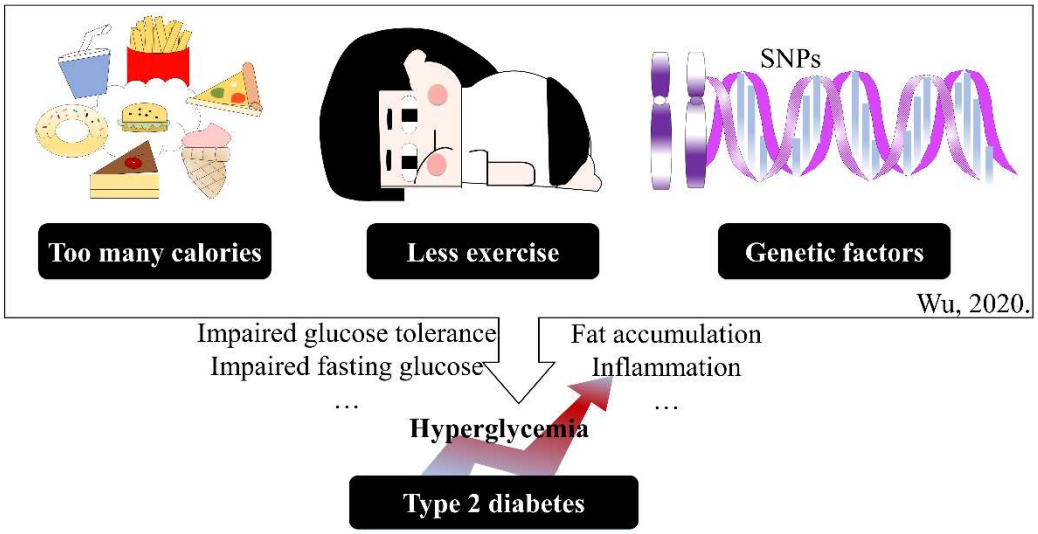


Figure 1. Causes of T2D.

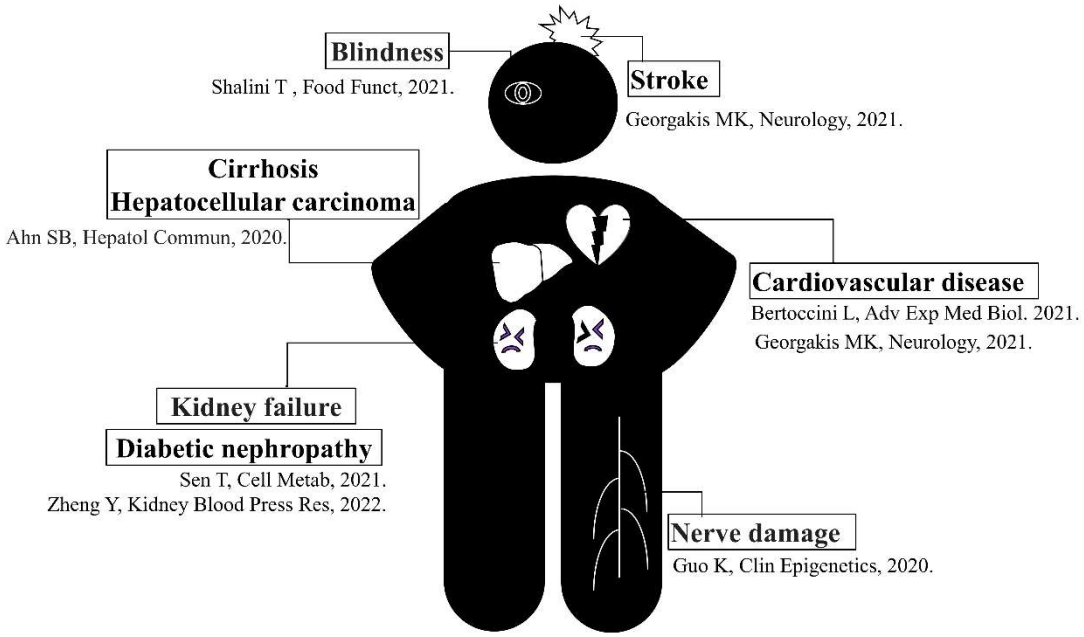


Figure 2. Damages of T2D.

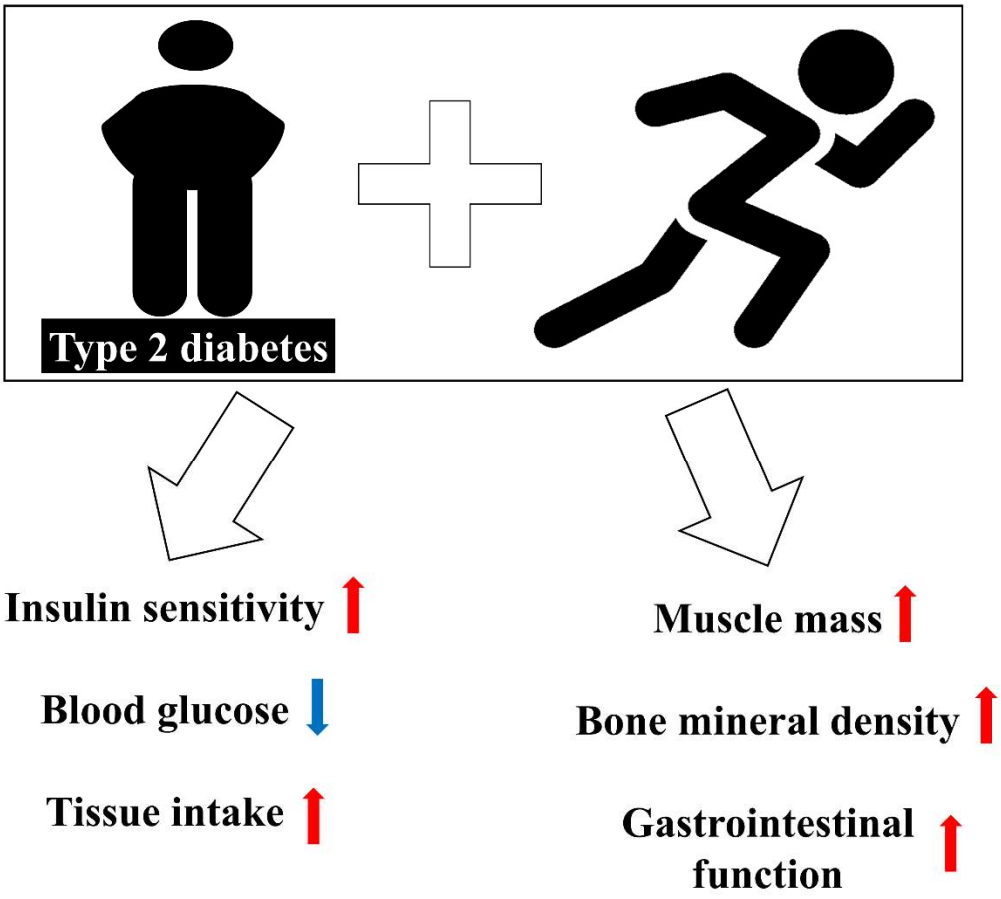


Figure 3. Exercise is an effect intervention to treat T2D.

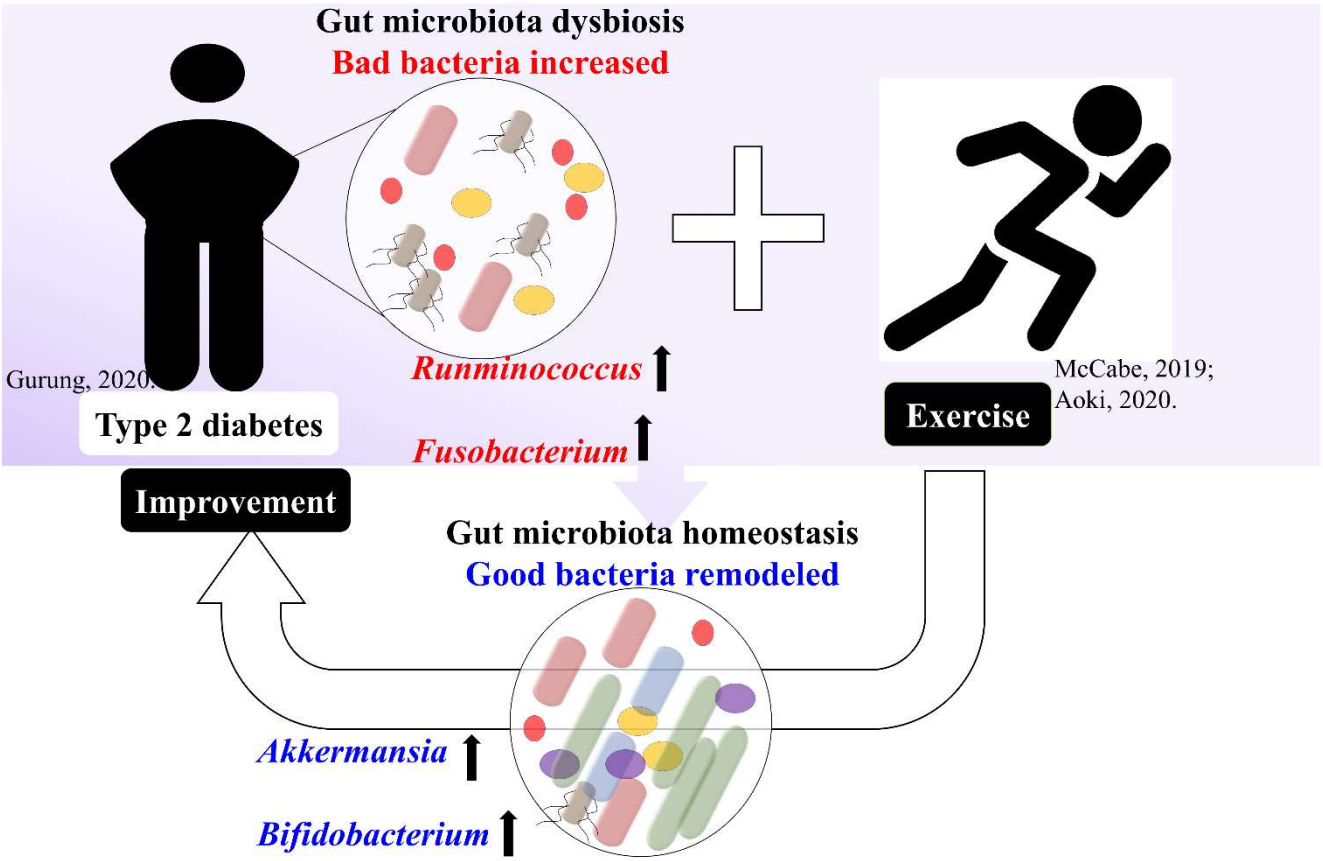


Figure 4. Exercise improves T2D by gut microbiota.

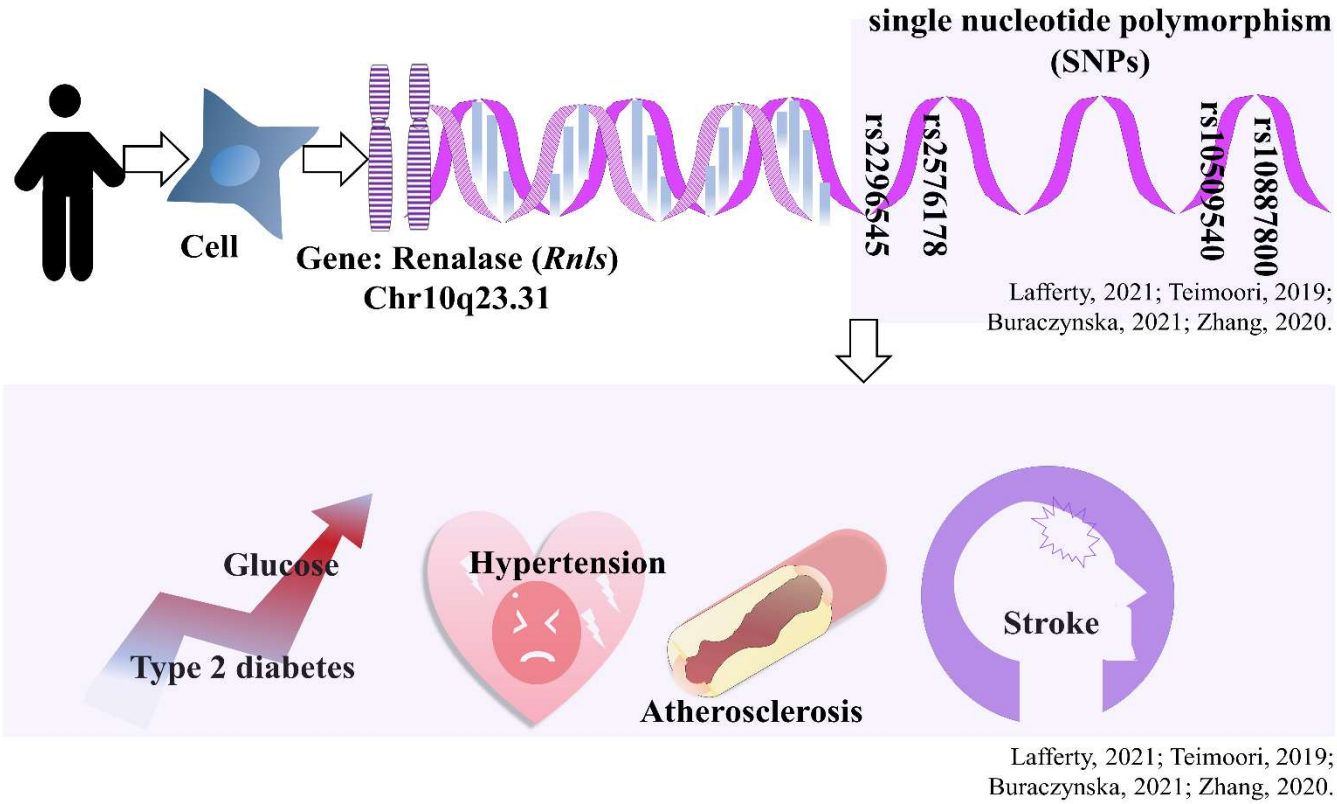


Figure 5. *Rnls* and metabolic diseases.

# II Previous Studies

1. Type 2 diabetes

1) Enteroendocrine L cells and Pc1/3 participate in glucose metabolism

Prolonged hyperglycemia as the main characteristic of type 2 diabetes (T2D) has around a lot of concentration [28-30]; therefore, effective regulation of glucose metabolism has become the key breakthrough point in treating T2D [31, 32]. In 1985, researchers discovered an incretin called glucagon-like peptide 1 (GLP-1). It is produced by the specific cleavage of proglucagon under the action of prohormone converting enzyme 1/3 (Pc1/3) in enteroendocrine L cells [33]. GLP-1 will interact with GLP-1 receptor which located in islet β cells for inducing insulin secretion and lower glucose levels [33-35]. The concrete physiological process is shown in Figure 6.

2) Type 2 diabetes with obesity

Obesity has the high risk to cause T2D [36]. One study examined the impact of obesity phenotypes on incident diabetes in 8430 men and 7034 women and came to the conclusion that ectopic fat obesity had the highest risk of incident T2D [37]. Adipose tissue inflammation and its possible connection to the obesity-related insulin resistance [38]. Adipose tissue becomes inflamed as a result of obesity's effects on the release of proinflammatory cytokines (such as interferon-γ, tumor necrosis factor-α, interleukin 6, transforming growth factor-β, monocyte chemotactic protein-1, and interleukin-1β), immune cells infiltration and insulin resistance. Lastly, encourage T2D aggravation [39, 40]. Additionally, due to the signaling pathway properties of the PI3K/AKT, which is vital for optimal metabolism, an imbalance might result in the development of obesity and T2D [41, 42].

2. Renalase and *Rnls*

1) Characters

Renalase is a flavoprotein oxidase that control the metabolism of blood pressure and catecholamine [23]. The human renalase gene (*Rnls*), which had a length of 31,000

base pairs, is found on Chr10q23.33. *Rnls* is expressed in several tissues, including the intestine, liver, and skeletal muscle according to the genomic result [23].

2) *Rnls*, renalase and T2D

*Rnls* has a closely relationship with the development of chronic diseases, such as diabetes, cardiovascular diseases [27, 43, 44]. Especially, the connections between single nucleotide polymorphism of Rnls and T2D were well revealed in recent years. Patients with diabetes exhibited the rs2576178 polymorphism generally, when compared with control individuals; those patients with T2D has high risk in hypertension and stroke if they has rs10887800 and rs2296545 polymorphisms [27, 34, 44, 45]. Additionally, gestational diabetes and the SNPs rs2576178 and rs10887800 were closely related. Another study revealed that people with diabetes had a greater GG genotype (rs2576178 and rs10887800) than healthy controls. What's more, one study pointed that renalase level of serum was higher in diabetes compared to control individuals. Another study showed that renalase level of serum was increased in diabetes with impaired renal function. Although we have not identified which *Rnls* polymorphism is connected to T2D, there is a close relationship between *Rnls* and T2D is confirmed at present.

3) Renalase, *Rnls* and exercise

In 2013, Bozena Czarkowska-Paczek et al. did one experiment to explore the relationship between renalase and exercise. their study found that rats who were given an endurance training may influence renalase expression in white muscle. In 2018, Tokinoya et al. found that rats who were given an acute exercise (10m/min or 30m/min, 30min) may increase renalase level of muscle[46]. With study goes on, Tokinoya et al. did another study. Rats were given a moderate intensity exercise (20m/s, 60min), then monitoring the changes of renalase in muscle and blood [47]. Results showed that moderate intensity exercise is able to elevate renalase level in muscle and blood. Despite feeding rat a high fat diet, a recent study by Tokinoya et al. demonstratd that

high intensity exercise training can enhance the *Rnls* level in skeletal muscle [47]. In conclusion, those studies showed that moderate-intensity exercise, acute exercise and endurance exercise in rat and mice both elevated renalase levels in the blood and skeletal muscle [46, 48]. Besides, aerobic exercise training is good for renal function by elevating *Rnls* level [49, 50].

4) Renalase, *Rnls* and gut

One research by Aoki et.al. investigated that *Rnls* overexpression is able to improve oxidative stress in Caco-2 cells by activating NF-κB transcription [51]. Moreover, renalase promotes cell survival in a lot of diseases models of animal (especially in gastrointestinal diseases), and the level of renalase was increased in animal and human cancer tissues [52]. These physiological processes depended AKT, MAPK, STAT3 signaling pathway activation [53].

3. Gut Microbiota

1) Three main types of gut microbiota

The gastrointestinal tract of mammals hosts a wide variety of microorganisms, which are collectively referred to as the gut microbiota [13, 22]. The gut microbiota is assembled in certain proportions, and the bacteria are mutually regulated and interdependent, forming an ecological balance in terms of quality and quantity [15]. The composition of intestinal bacteria is complex and there are many kinds of bacteria, but they can still be divided into three types [54].

The first is the symbiotic bacteria, mainly Bacteroides, *Clostridium*, *Bifidobacterium*, and *Lactobacillus*. These names are familiar. The probiotics that are overwhelming in various products now refer to the latter two. There are many prebiotics or prebiotics that are used to supplement or stimulate the growth of *Bifidobacterium*. These bacteria are the most powerful, accounting for more than 99% of the intestinal microbiota. They form a good cooperative relationship with people, assist in the digestion of various foods, and protect our intestinal tract [54].

The second type is conditional pathogenic bacteria, mainly including Enterococcus and Enterobacteriaceae. There aren't many of these guys, but they're a destabilizing factor in the gut. When the intestinal tract is healthy, the symbiotic microbiota is overwhelmingly dominant, and the conditional pathogenic microbiota is very safe; but if the symbiotic microbiota is destroyed, these guys will cause a variety of intestinal diseases [54].

The third type is pathogenic bacteria, such as Salmonella, pathogenic E. coli. They are destroyers of health. They do not belong to the intestinal tract, but once they enter the intestinal tract by mistake, they will cause trouble, causing diarrhea, food poisoning [54].

2) Tools for gut microbiota analysis

A full understanding of the gut microbiota is particularly important for the promotion of organismal health. There are many tools available today for the analysis of the gut microbiota, the most widely used being high-throughput sequencing of the 16S rRNA gene, which is commonly found in bacterial cells and is located in the small ribosomal subunit (~1540 bp) of the bacterial genome [55, 56]. The conserved regions can be used to design primers for amplification of the target fragment, while the highly variable regions can be analyzed to identify the bacterial species. Therefore, the 16S rRNA gene is considered as the most suitable for bacterial phylogenetic studies and species taxonomic identification. The main regions currently used for deep sequencing of the 16S rRNA gene are the V4 region, the V3-V4 region, and the V4-V5 region. DNA samples of tested environmental microorganisms are subjected to PCR amplification, library preparation, library quality control, quantification of their designated regions, and sample differentiation using set TAG sequences [57]. The Illumina Hiseq 2500 high-throughput sequencing platform was used to sequence the tested libraries [58]. The experimental process is shown in the Figure 7. The 16S analysis process includes: the Paired-end (PE) reads obtained from Hiseq/Miseq sequencing are spliced into one sequence, the target sequence is filtered for quality control, the filtered sequence is compared with the reference database, and the chimeric sequence is removed to obtain the final optimized sequence [58]. Based on the

optimized sequences, OTU clustering analysis and species taxonomic annotation were performed, diversity index analysis was performed based on OTU clustering results, and species structure analysis and species difference analysis were performed based on taxonomic information [58]. The detailed analysis flow is shown in the Figure 8.

3) Routine analysis of gut microbiota

OTU clustering and species annotation

OTU (Operational Taxonomic Units) is a hypothetical taxonomic unit in phylogenetic analysis or population genetic studies, where the distance metric or similarity between two-two different sequences is calculated by a certain distance metric, followed by setting a specific classification threshold, obtaining a distance matrix under the same threshold and performing a clustering operation to form different classification units [59].

The purpose of OTU clustering is summarized as follows [59]: 1. Each OTU (97%) corresponds at rank to a species/genus; 2. To save computational resources by selecting one representative sequence per OTU for subsequent analysis; 3. To reduce errors introduced during PCR or sequencing (erroneous sequences are more similar with their source sequences and will cluster into an OTU). Based on a 97% sequence similarity level, OTU clustering analysis was performed using the Uclust method in the QIIME package. The OTUs of each sample were then annotated for species taxonomy based on the Silva.

Species structure analysis

The taxonomic results of all samples were counted at each level of the phylum, order, family and genus [60]. Differences in species composition between samples were compared using cumulative histograms based on the top fifteen species in abundance [60]. What's more, based on the species abundance information for each sample at the genus level, the top 50 genera in terms of abundance were selected and the samples and species were clustered based on the abundance information for each sample to create a heatmap [60]. It is easy to see how high or low the corresponding species content of the sample is.

Alpha Diversity Analysis

Alpha diversity refers to the diversity within a given area or ecosystem [61]. The diversity index is a composite indicator of the abundance and evenness of microorganisms in a sample [61, 62]. Alpha diversity analysis mainly includes the calculation of diversity indices such as Shannon's diversity index, Simpson's index and Chao1 richness index [62].

Chao1: The index for estimating the number of OTUs contained in a community using the chao1 algorithm, commonly used in ecology to estimate the total number of species, was first proposed by Chao in 1984.

The Shannon-Wiener index was proposed by Shannon, C. E. and Weaver W in 1948. An index reflecting the microbial diversity in a sample, a curve is constructed using the microbial diversity index for each sample at different sequencing depths, thus reflecting the microbial diversity of each sample at different sequencing quantities.

Beta Diversity Analysis

Beta Diversity is a comparative analysis of the composition of microbial communities among samples/groups of samples [63, 64]. It can be calculated as distance between samples using the abundance information of OTUs, or as phylogenetic relationships between OTUs.

UniFrac is a distance measure for comparing biomes that incorporates phylogenetic distances in its calculations, measuring the differences between two different environmental samples based on the length of the evolutionary tree branches constructed [64]. UniFrac analysis is divided into two metrics, weighted unifrac and unweighted unifrac, which differ in whether they take into consideration the relative abundance of sequences from different environmental samples. Unweighted UniFrac only takes into consideration variation in the presence or absence of species, so a distance of zero in the results indicates that the species of OTUs are the same between the two microbial communities. In contrast, Weighted UniFrac takes into consideration both species presence and species abundance, and a distance of 0 indicates that the species and number of OTUs are the same between communities.

PCoA analysis

Principal Coordinate Analysis (PCoA) is a visualization method to study the similarity or difference of data, based on a distance matrix to find the principal coordinates, and a series of eigenvalues and eigenvectors are sorted to select the top eigenvalues, effectively finding the most The relationship among the samples is described by selecting the top features through a series of eigenvalues and eigenvectors, effectively identifying the most "dominant" elements and structures in the data [64, 65]. The unifrac distances among the samples were first calculated by random sampling, and then a two-dimensional PCoA plot was drawn based on the distance matrix, with the closer the samples were to each other (e.g. the more similar the abundance and composition of the species), the closer they were to each other in the PCoA plot.

LEfSe analysis

LEfSe analysis, or LDA Effect Size analysis, is an analysis used to discover high-dimensional biomarkers and reveal genomic features using the non-parametric factorial Kruskal-Wallis (KW) sum-rank test (non-parametric factorial Kruskal Wallis sum-rank test) to detect features with significant abundance differences and to find taxa that differ significantly from each other in abundance [66]. Finally, LEfSe used linear discriminant analysis (LDA) to estimate the magnitude of the effect of each component's (species') abundance on the differential effect. The ability to find biomarkers that are statistically different among groups, e.g. species that differ significantly among groups. The LDA scores of the different groups of microbial taxa with significant effects are counted by LDA analysis (linear regression analysis), showing the species with LDA scores greater than a set threshold, e.g. biomarkers with statistically significant differences. the length of the bar chart represents the size of the effect of the species with significant differences.

4. The relationship among GM, T2D, exercise

1) Microbiota and its metabolites with obesity, T2D

The key element in the development of metabolic syndrome is the gut microbiota (GM). Generally speaking, obese individuals have a significantly different GM composition from control individuals; such as *Oscillibacter*, *Akkermansia*, *Alistipes,* and *Faecalibacterium* were lower [67, 68]. According to the latest statistics, bacteria of genera *Akkermansia*, *Bifidobacterium*, and *Faecalibacterium* have a negative relationship with T2D, while bacteria of genera *Runminococcus*, *Fusobacterium*, and *Blautia* have a positive relationship with the progression of T2D [69].

Unbalanced gut microbiota can affect intestinal permeability, which will aggravate the progression of T2D [70]. Some bacteria can help reduce leakage in the gut by creating tighter junctions in our cells, or by preventing the disruption of the mucus layer, such as *Lactobacillus* [71]. The mucus layer is a thin layer that sits on top of the inner layer of the intestine. The tight junctions are small proteins between the cells in the gut that prevent leakage of particles. Meanwhile, some microbiota can influence blood glucose level and control the digestion of carbohydrate, such as bacteria that produce butyric acid from the digestion of dietary fiber [72, 73]. Butyric acid is a fatty acid that plays an important role in homeostasis and metabolism in the body. Some microbiota may affect the production and release of gut hormones, and butyric acid can also have a significant impact on this [18, 74]. Studies have shown that gut microbiota are the important factor in triggering insulin resistance, and *Akkermansia* have become a focus of research in patients with type 2 diabetes and some obese patients, with newly diagnosed type 2 diabetics and pre-diabetics beginning to have lower levels of *Akkermansia* [18]. This decrease in abundance is a biomarker of glucose intolerance.

2) GM with endocrine L cells' function

The gut is the habitat of the microbiota colonizing the gastrointestinal tract and endocrine L cells [16, 75, 76]. According to the earlier research, enteroendocrine L cells are multiplied by colonized microbiota and their metabolites to improve glucose homeostasis [77]. Additionally, probiotics, such as *Bifidobacterium* and *Lactobacillus* strains, enhance insulin secretion and exert glucose regulatory effects by upregulating the activities of Pc1/3 [78]. Metabolites derived by GM are also involved in glucose

regulation in different ways. Enteroendocrine L cell density was enhanced by short-chain fatty acids (SCFAs), meanwhile, GLP-1 production was also elevated [79, 80]. Secondary bile acids promote L cell differentiation via 5-hydroxytryptamine (5-HT) signaling [81]. Representative previous study is showed in Figure 9.

3) GM, metabolites and exercise

GM of athletes is different from sedentary controls, they have higher levels of metabolites such as SCFAs [82]. Exercise has the power to regulate the interaction between host and gut microbiota [83]. Exercise has been shown in certain studies to help mice with HFD regain their GM homeostasis by lowering the Firmicutes/Bacteroidetes ratio [83, 84]. In May 2020 Maria Kulecka's team studied "Differential gut microbiota in endurance athletes and sedentary people" [85]. The results showed that athletes had higher microbiota species richness, higher abundance of *Prevotella* and lower abundance of *Bacteroidetes* compared to sedentary people, and that strains enriched in athletes were involved in fiber fermentation. Dr. Lucy Mailing of the University of Illinois, who conducted a similar experiment on the general population without exercise habits, asked the volunteers to increase their weekly exercise without changing their diet [21]. The experiment found that the volunteers showed a large increase in short-chain fatty acid-producing microbes after exercise, especially in people with a slim body type. However, once people stopped exercising, their gut microbiota returned to the state it was in before the study. An international team of researchers led by Nanyang Technological University in Singapore found that microbiota in the gut can help muscle growth and enhance muscle function, opening new doors for intervention in age-related skeletal muscle loss [86]. The results showed that mice with gut microbiota had stronger skeletal muscle and could generate more force compared to germ-free mice. And when they re-transplanted gut microbiota from standard laboratory mice into germ-free mice, muscle growth and function were partially restored in the germ-free mice, demonstrating the link between gut microbiota and skeletal muscle mass. Another study showed that healthy gut microbiota can also convert certain substances in food into metabolically active regulatory factors that

affect muscle function as the way to then improve exercise capacity [87]. This is also how exercise affects the health of the body through the gut microbiota.

5) The signaling pathway activated by GM and its metabolites

Metabolic signaling pathways which improve inflammation and glucose/lipid metabolism such as AKT and MAPK, are influenced by GM metabolites, including secondary bile acids, SCFAs, trimethylamine, farnesoid X receptor [88-90]. According to a study, *Akkermansia muciniphila* increases mice's thermogenesis, which causes them to lose wight and enhance the GLP-1 release to maintain glycemic homeostasis by P9 [18]. The results of a study by Larsen et al. found a significant decrease in the number of thick-walled bacteria and an increase in the number of Gram-negative bacteria in the fecal intestinal flora of type 2 diabetic patients [91]. A recent study on the gut microbiota of Chinese people [92], which was divided into 3 groups according to blood glucose level, revealed an increase in the number of *Aspergillus* and a decrease in the number of *Bacteroidetes* in the intestine of type 2 diabetic patients compared to patients with pre-diabetic status and normal subjects. *Streptococcus* was most abundant in normal subjects, reduced in number in patients with pre-diabetic status and more so in type 2 diabetics. The level of *Megamonas* was higher than normal subjects. It was also found that the abundance of β-deformed bacteria increased significantly with diabetes and was positively correlated with blood glucose [92]. Type 2 diabetic patients had significantly lower numbers of *Bifidobacterium* and higher numbers of enterococci than healthy individuals [92]. The gut microbiota of diabetic patients showed a decrease in butyric acid producing bacteria and an increase in opportunistic pathogenic bacteria [71].

4) GM and host genes

It has been documented that the host and gut microbiota have an adaptation interaction [93]. Studies revealed that host gene expression has been shown in genome-wide association analysis to have an impact on the species and composition of GM

organisms [94, 95]. However, relatively few genes have been uncovered until now. The connection between host genes and GM composition required more study on.

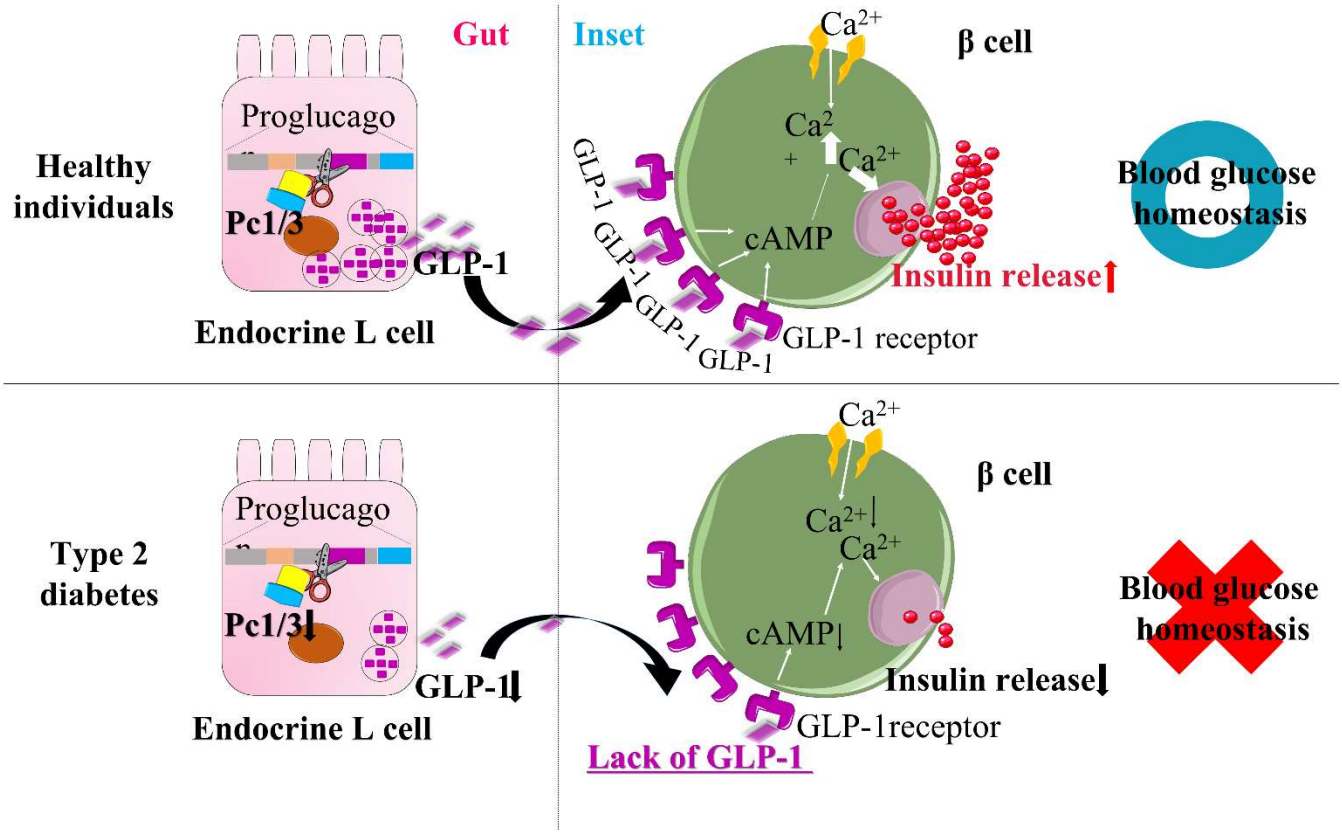


Figure 6. Comparation of endocrine L cells function between healthy individuals and type 2 diabetes.

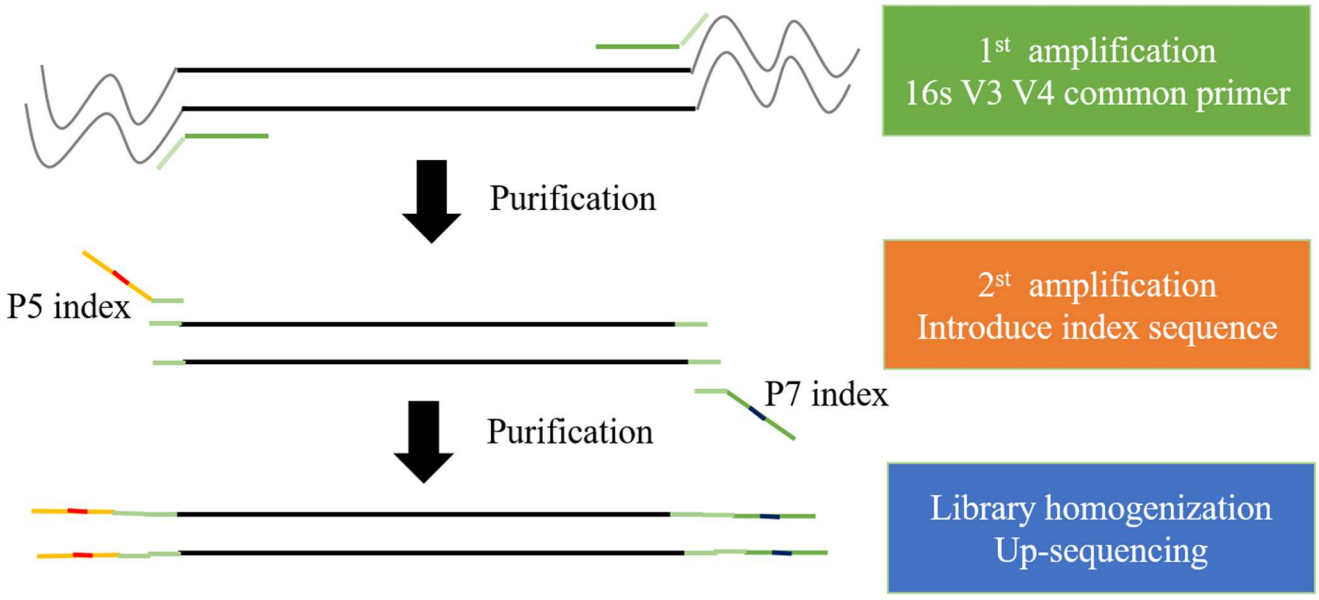


Figure 7. The simplified experimental process of 16s high throughput sequencing.

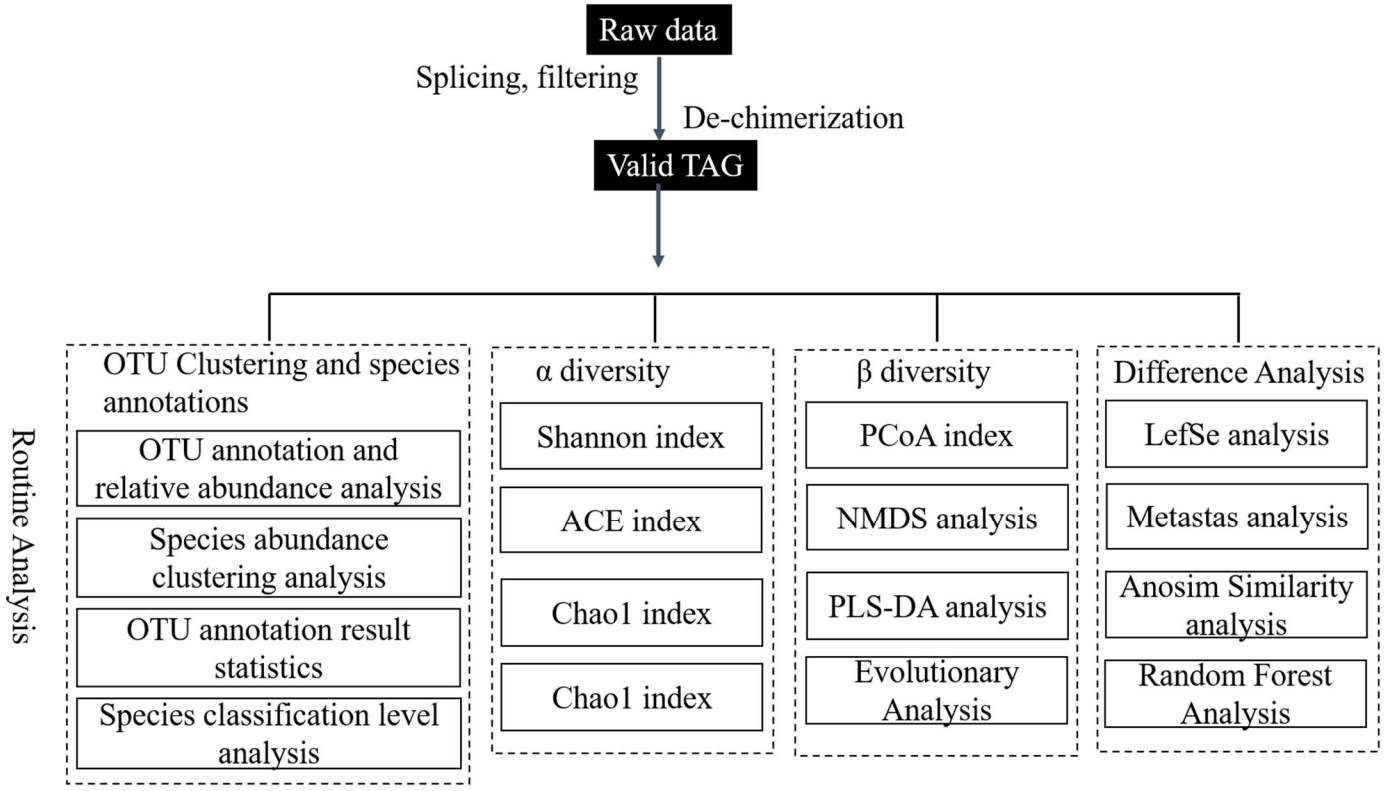


Figure 8. The analysis process of 16s high throughput sequencing.

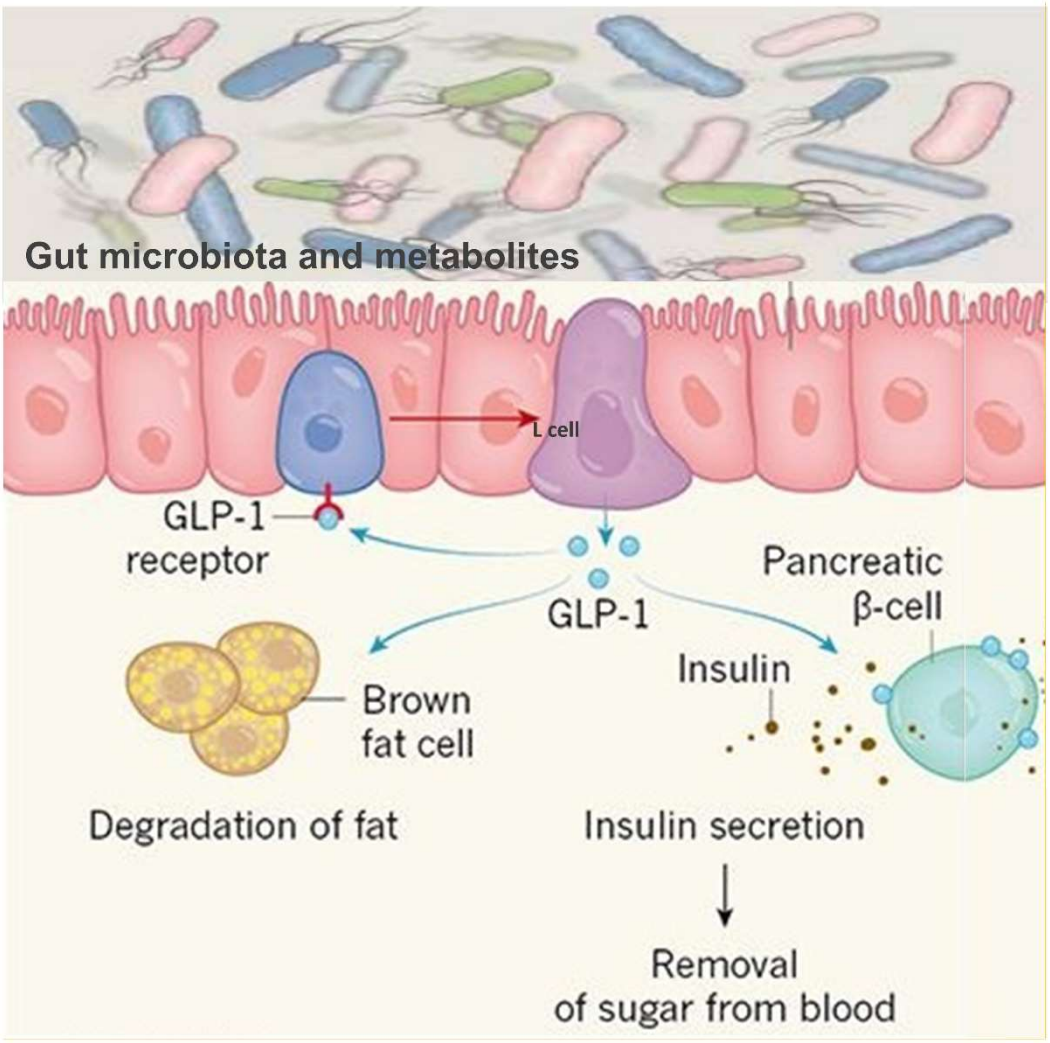


Diabetes, Fiona M. Gribble,2012.

Figure 9. Gut microbiota and L cells function.

# III Aim

Through previous studies, I have gained insight into the mechanisms of gut microbiota on exercise, type 2 diabetes and glycemic regulation, and the influence of host gene on the composition of gut microbiota. To demonstrate the function of *Rnls* on exercise-enhanced glucose homeostasis by gut microbiota, I designed my doctoral thesis. My study focused on *Rnls* knockout mice and its relationship with gut microbiota, type 2 diabetes, and exercise-enhanced glucose homeostasis. Now involved in diet-induced animal model. Diet-induced models refer to animal models made from animal strains with a genetic susceptibility to obesity and diabetes as model organisms, using a high fat diet as a trigger [96-98]. It is similar to human pathogenesis and is highly reproducible and simple to manipulate [98]. The male C57BL/6J is the most widely used background animal for obese type 2 diabetes [99]. This strain of mice has the genetic predisposition to develop diabetes later in life after obesity. When building a model, success is usually judged by indicators of metabolic syndrome disputes, such as body weight, glucose tolerance, high density lipoprotein (HDL), low density lipoprotein (LDL), and total cholesterol [100, 101]. There have also been many studies in this area and usually fatty degeneration of the liver could be seen after 8 weeks when fed a high-fat diet alone and an increase in all indices can be seen after 10 weeks [102]. Also, with regarding to the *Rnls* knockout mice, which was also generated on a C57BL/6J background, the *Rnls* knockout (B6;129S1-Rnls$^{tm1Gvd}$/J mice) was commissioned from Jackson Laboratory, and could be stably bred and then used to carry out the experiments in this study. Genotype of *Rnls* knockout in mice was defined by PCR-Agarose gel electrophoresis [103]. The representative picture was showed in Figure 10.

Another important thing of animal experiment is replicates of samples. Replicates of samples are important for the experimental design of sequencing and subsequent analysis of information. Setting up multiple sample replicates serves several purposes.

1) It can eliminate intra-group errors and detect outlier samples: the presence of abnormal samples can seriously affect the accuracy of sequencing results, and subsequent information analysis can identify abnormal samples and exclude them.

2) Enhances the reliability of the results. The more samples sequenced, the better the ability to reduce background variation and thus increase the reliability of the results.

In general, a minimum of 5 biological replicates per group is recommended for model animals with small differences between individuals (e.g. rats, mice, chickens, etc.), and 10 biological replicates are generally recommended.

In the case of samples of human intestinal feces, due to the large differences between individuals (e.g. effects of environment, diet, genetic conditions, health status, age, sex, etc.), a larger sample size of no less than 30 samples per group is recommended (too few samples are not convincing and statistical differences may not be significant). If multiple samples are mixed for library sequencing, multiple samples are synthesized into one sample and multiple replicates are still required.

Above all, this study hypothesized that *Rnls* knockout influence exercise-enhanced glucose tolerance by the diversity of GM. Therefore, I monitored the blood glucose level and microbiota changes from mice model under different lifestyle intervention. Notably, I also did in vitro experiment to identify the underlying mechanism. The whole thesis structure was showed in the following picture (Figure 11).

<Study 1>

"Exploring the mice with or without *Rnls* knockout on BG level under different interventions"

Whether *Rnls* knockout will cause the dysfunction of BG is still unknown. Hence, I established mice model by treating with either a normal diet (ND), high fat diet (HFD) or treadmill training. Further, glucose tolerance of mice was evaluated by intraperitoneal glucose tolerance test (IPGTT), and use glucometer to detect the BG level.

<Study 2>

“Comparing the GM composition of mice with or without *Rnls* knockout under ND or HFD”

Study 1 suggested that *Rnls* knockout has a negative impact on BG level under HFD, and exercise could not alleviate such a negative impact. Feces were collected for detecting the difference in GM by 16s high through-put sequencing.

<Study 3>

“Illustrating the metabolites from GM to regulate the function of enteroendocrine L cells”

According to study 2, *Rnls* knockout changed the GM composition, especially the proportion of *Bifidobacterium*. Hence, metabolites of microbiota were extracted from feces to illustrate the influence on L cells. I used STC-1 cell line to imitate L cell bioactivity in vitro, explored the differences on cell proliferation and cell signaling pathway.

This doctoral thesis explored the importance of *Rnls* knockout on exercise-enhanced glucose tolerance by GM through above studies.

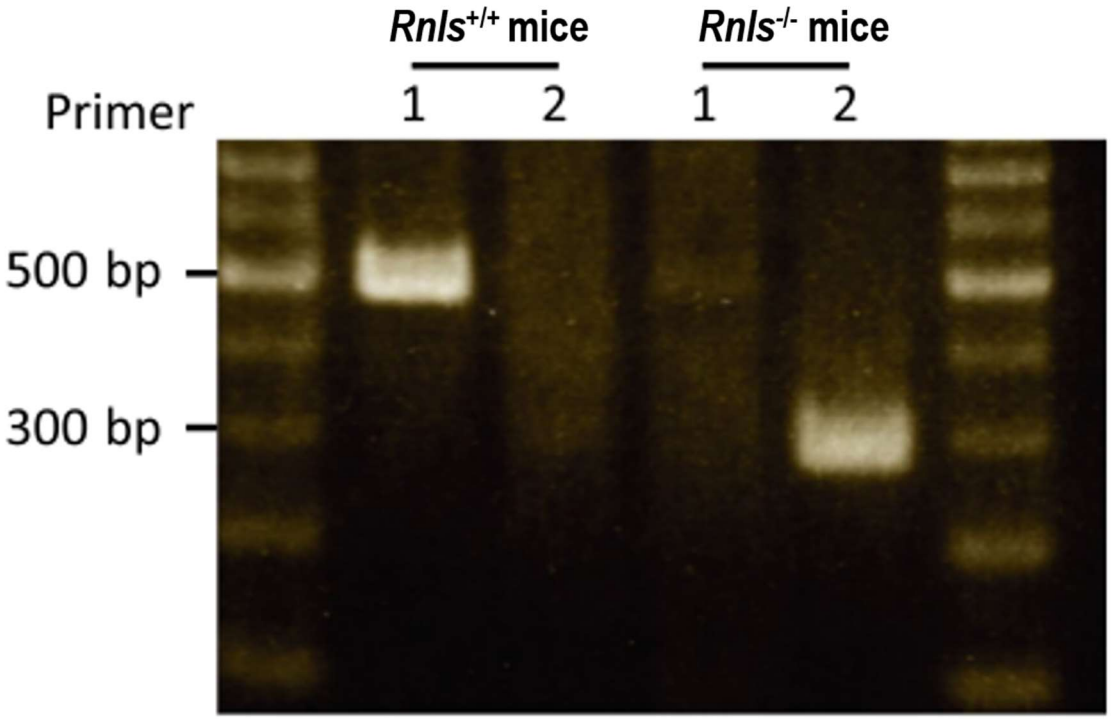


Figure 10. Genotype of *Rnls* in mice.

Primer 1, the array that is amplified at portion of exon 1–4; Primer 2, the array that is amplified at portion of resistance gene of neomycin. Both sides showed markers. $Rnls^{-/-}$ mice*, Rnls* knockout mice*;* $Rnls^{+/+}$ mice, wild type mice.

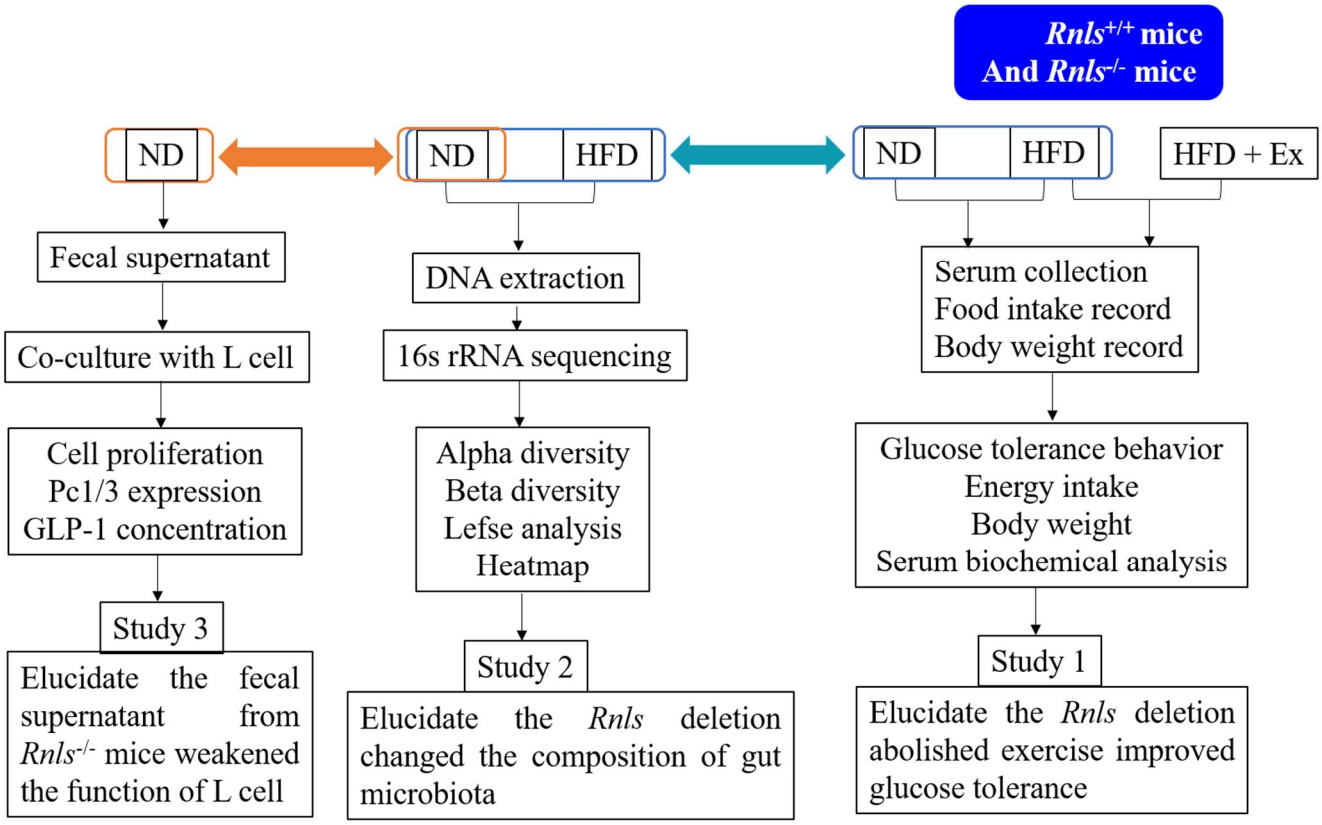


Figure 11. Profile map of doctoral thesis.

# IV study 1

Exploring the BG level in mice with or without *Rnls* knockout under different interventions.

## 1. Aim

This study hypothesized that the mice with *Rnls* knockout will affect the BG level. The purpose of this study was to demonstrate how *Rnls* affected BG under various interventions.

## 2. Material and methods

*Animals and experimental design*

B6;129S1-Rnlstm1Gvd/J mice were obtained from the Jackson Laboratory. Identification of wild-type ($Rnls^{+/+}$) and *Rnls* knockout ($Rnls^{-/-}$) mice was done using Polymerase Chain Reaction as described previously [104]. The animals were housed in a room at 12-h/12-h light-dark cycle conditions and the temperature was maintained at the range of 20°C–26°C. After acclimatizing for 7 days $Rnls^{+/+}$ mice and $Rnls^{-/-}$ (n=5/group, male, 4-weeks-old) mice were divided into groups by randomization. For a total duration of 8 weeks, mice were fed with ND (Cat#MF, Oriental Yeast, Itabashi, Tokyo, Japan) with free access to water (Figure 12). BG level of both groups were evaluated. Next, in order to reveal whether *Rnls* knockout affects blood glucose level on HFD and whether exercise improves blood glucose level of *Rnls* knockout mice with HFD $Rnls^{+/+}$ and $Rnls^{-/-}$ (male, 4-weeks-old) 10 mice each were used. These mice were randomly divided into 4 groups; $Rnls^{+/+}$-HFD (n = 5), $Rnls^{-/-}$-HFD (n = 5), $Rnls^{-/-}$-HFDEx (exercise) (n = 5) and $Rnls^{+/+}$-HFDEx (exercise) (n = 5). These mice were fed with HFD (Cat#D12492, 60 kcal% fat; Research Diets, New Brunswick, NJ, USA) with free access to water Table 1 shows the composition fatty acids of HFD. Exercise group was given a moderate intensity treadmill training (20m/min, 5days/per week) from the

fourth week of the experimental period. The concrete experimental design is showed in Figure 13.

A previous study reported that feeding mice with for 8-12 weeks with HFD (40%–60% fat calories) will induce obesity [90]. Therefore, in this study HFD mice we also given 60% fat calories diet for period of 8 weeks. We measured body weight (BW) of mice weekly. Additionally, we performed intraperitoneal glucose tolerance test (IPGTT) on the 7th week of the study, followed by an intraperitoneal insulin tolerance test (IPITT) on 8$^{th}$ week of the study. All protocols of this study were conducted according to the recommendations of animal work approved by the Animal Subjects Committee, University of Tsukuba, Japan (approval number: 21–027).

*Energy consumption*

In this study, two different types of diets were ultilized: a normal diet; (ND; Cat#MF, Oriental Yeast, Itabashi, Tokyo, Japan), and a high-fat diet (HFD; Cat#D12492, 60 kcal% fat; Research Diets, New Brunswick, NJ, USA). Divide the dry food weight taken by the cage by the number of mouse animals, calculate the dry food weight per diem, and determine the energy value. Multiply the number to get the amount of energy consumed per day. Energy coefficient is 60 kcal% 5.24cal/g, normal diet 3.59cal/g.

*Body weight*

We measured the body weight (BW) of mice weekly (0.1g changes also included), throughout the study ending in 8$^{th}$ week. The weekly average body weight changes were compared among the groups to analyze the impact of diet and exercise.

*IPGTT and IPITT*

On the seventh week, the IPGTT was run. Briefly, after fasting mice for the previous night, tail tip was cut and use a glucometer (ACE-Quick, ACUU-CHEK, Roche, Basel, Switzerland) to determine the baseline blood glucose level (at time point 0). After that, the mice received an intraperitoneal injection of glucose (20% D (+)-glucose, 2 mg/g BW). At 15, 30, 60, and 120 minutes, blood from tail was drawn and

measured. IPITT was done at the eighth week with fasting 4 hours, tail tip was cut and use a glucometer (ACE-Quick, ACUU-CHEK, Roche, Basel, Switzerland) to determine the baseline blood glucose level (at time point 0). After that, the mice received an intraperitoneal injection of insulin (0.75 U/kg BW, Humulin-R; Lilly Research Labs, Indianapolis, IN, USA). At time points 15-, 30-, 60-, and 120-min post-injection, blood from tail was drawn and measured.

*Biochemical analysis*

The Oriental Yeast Co., Ltd. (Itabashi, Tokyo, Japan) examined the following general plasma biomarkers: triglycerides (TG) (mg/dL), high density lipoprotein-cholesterol (HDL-C) (mg/dL), total protein (TP) (g/dL), low density lipoprotein-cholesterol (LDL-C) (mg/dL) and total cholesterol (TC) (mg/dL).

*Mice euthanasia*

At the completion of the experimental time, the mice were put to death via cervical dislocation under general anesthesia from isoflurane inhalation. Mice's behavior was observed closely during the anesthesia process. The cervical dislocation was performed only after the mice's respiratory frequency was decreased and depth increased. After euthanasia and collection of various samples, mice were placed in the −20 °C freezer of the animal carcass disposal room.

*Statistical analysis*

Data are presented as mean ± SD (standard deviation). Student's t-test was performed for statistical analysis using GraphPad Prism 8.0.1 (GraphPad Software. Inc). The p-value of $<0.05$ was considered statistically significant.

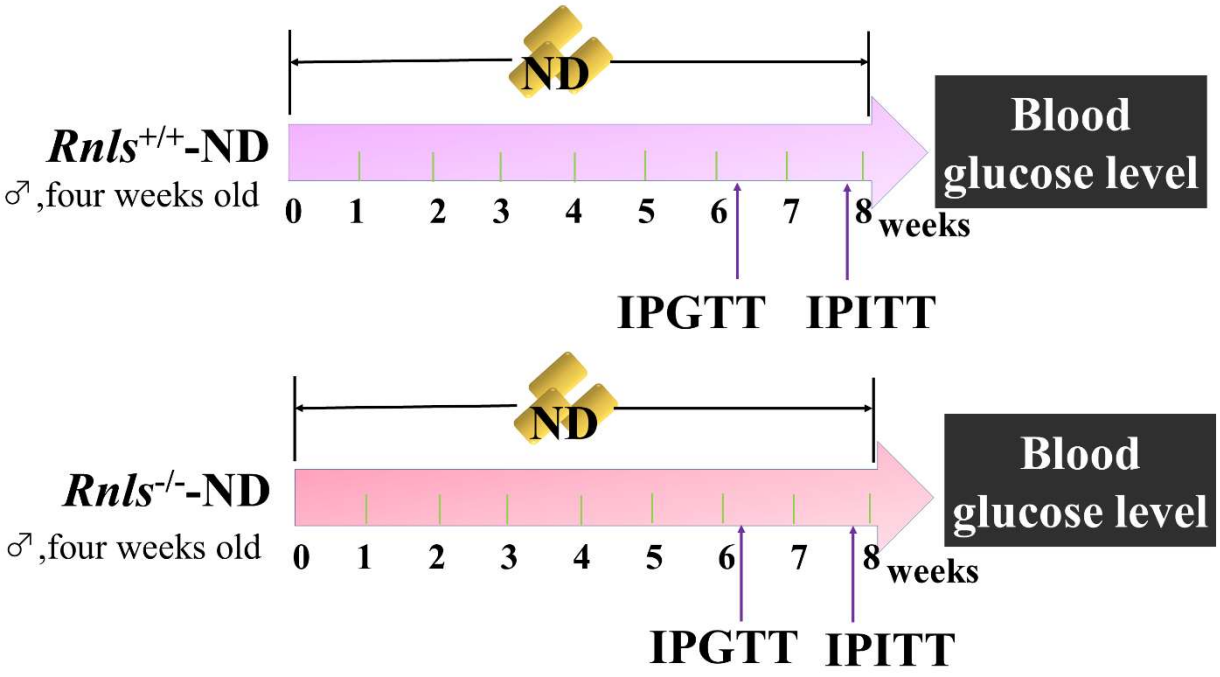


Figure 12. Experimental design for study 1-1.

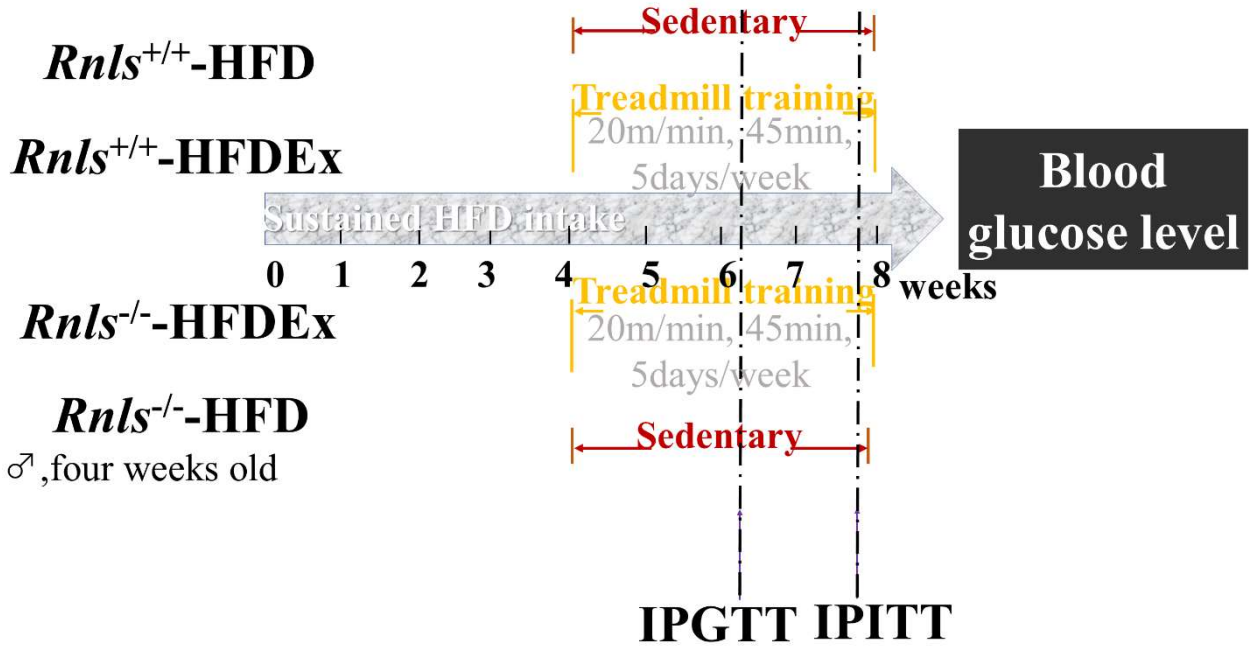


Figure 13. Experimental design for study 1-2.

# 3. Results

*Glucose tolerance had no different in the two groups*

GTT under ND, any difference at all time periods was not found (Figure 14A). Absolutely, there was no difference of AUC (Figure 14B). Similar results like GTT, ITT of *Rnls*$^{-/-}$ and *Rnls*$^{+/+}$ mice also had no difference under ND at any time points (Figure 14C), there was also no difference of AUC (Figure 14D). In addition, I also recorded the weekly energy consumption of one mouse (Figure 14E). Unfortunately, I did not observe any difference in energy consumption. BW recorded weekly showed that ND has similar effect on body weight increase of *Rnls*$^{-/-}$ and *Rnls*$^{+/+}$ mice (Figure 14F).

*Plasma biochemical parameters of Rnls*$^{-/-}$ and *Rnls*$^{+/+}$ mice *under ND*

The biochemical indices of fat content (e.g., TP, TG, TC, VDL-C, HDL-C) reflect the physiological and health status in clinical and disease animal models were ecaluated in the two groups (*Rnls*$^{+/+}$-ND, *Rnls*$^{-/-}$-ND). Results were showed by Figure 15. All the biochemical indices were no difference between *Rnls*$^{-/-}$ and *Rnls*$^{+/+}$ mice under ND. It indicated that *Rnls* knockout did not change these parameters under ND.

*HFD impaired glucose tolerance and exercise has no ability to recover it in Rnls*$^{-/-}$ mice

To evaluate the influence of HFD and exercise in *Rnls*$^{-/-}$ and *Rnls*$^{+/+}$ mice on glucose tolerance, IPGTT and IPITT were conducted. In *Rnls*$^{-/-}$-HFD and *Rnls*$^{-/-}$-HFDEx group, higher BG at 60 and 120 min than other groups (Figure 16A). In other words, exercise could not rescue the high glucose level of *Rnls*$^{-/-}$ mice (*Rnls*$^{-/-}$-HFDEx group) (Figure 16A). Similarly, the AUC for IPGTT in *Rnls*$^{-/-}$-HFD mice is highest among the four groups (Figure 16B), and the AUC for IPGTT of *Rnls*$^{-/-}$-HFDEx group had significant difference that *Rnls*$^{+/+}$-HFDEx group. Subsequently, IPITT was conducted. Regrettably, IPITT of *Rnls*$^{-/-}$ and *Rnls*$^{+/+}$ mice under HFD or HFDEx did not exhibit any difference at any time points, although HFD seemed to have high glucose level at the same time point (Figure 16C). Similarly, there was no difference of AUC in the four groups (Figure 16D). I additionally evaluated one mouse's weekly

energy consumption (Figure 16E). Unfortunately, any difference was not seen in energy consumption. Both *Rnls*$^{+/+}$ and *Rnls*$^{-/-}$ mice's BW statistics at the conclusion of experiment demonstrated that the HFD raised BW while exercise decreased BW (Figure 16F). Additionally, under the same intervention, there was not any variation in BW between *Rnls*$^{-/-}$ and *Rnls*$^{+/+}$ mice.

*Plasma biochemical parameters of Rnls*$^{-/-}$ and *Rnls*$^{+/+}$ mice *with or without exercise under HFD*

The biochemical indices of fat content (e.g., TP, TG, TC, VDL-C, HDL-C) reflect the physiological and health status in clinical and disease animal models were elevated in the four groups (*Rnls*$^{+/+}$-HFD, *Rnls*$^{-/-}$-HFD, *Rnls*$^{+/+}$-HFDEx, *Rnls*$^{-/-}$-HFDEx group). All the biochemical indices showed in Figure 17 were no difference between *Rnls*$^{-/-}$ and *Rnls*$^{+/+}$ mice under the same intervention.

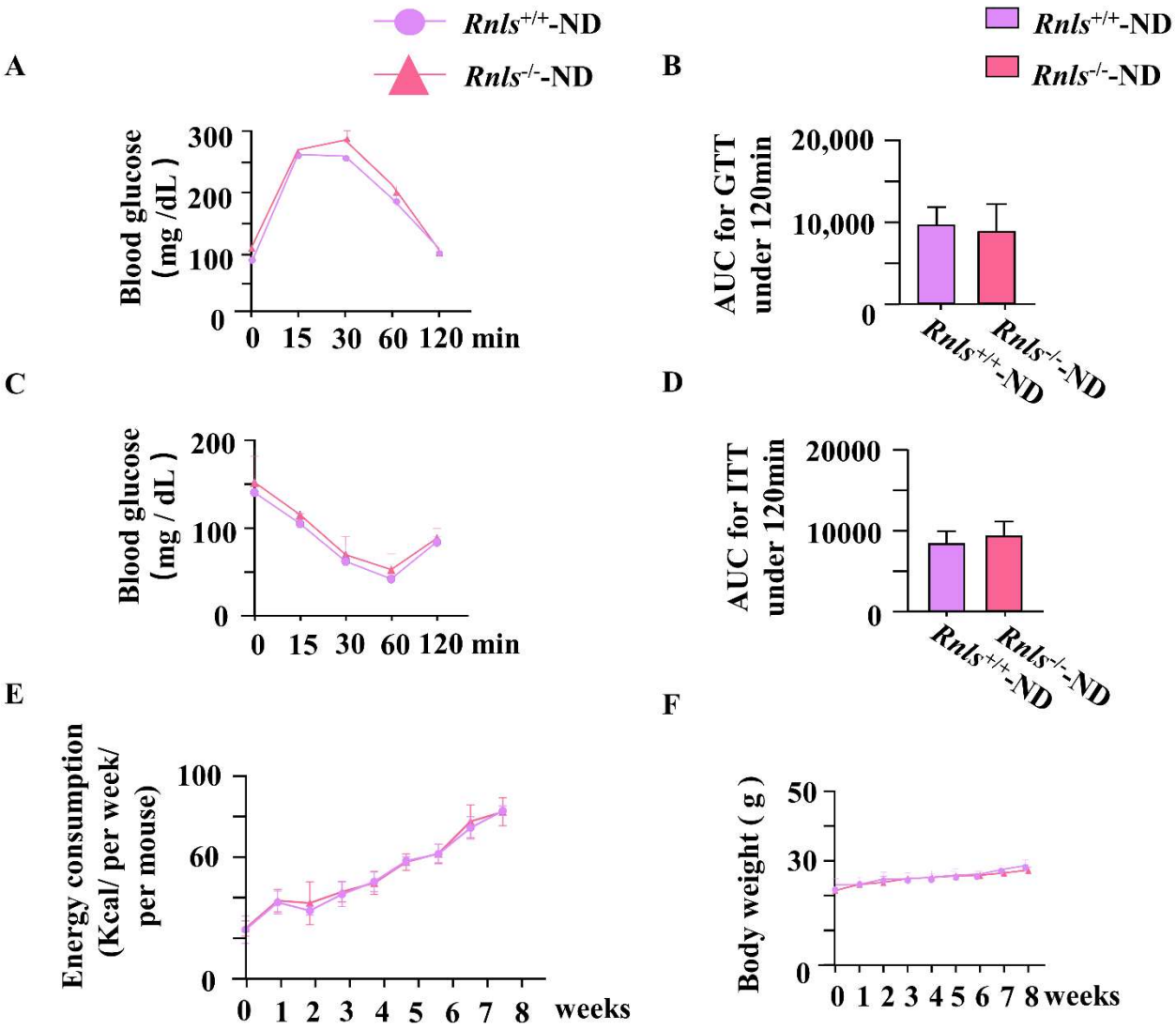


Figure 14. Phenotype of *Rnls*$^{-/-}$ and *Rnls*$^{+/+}$ mice under ND.

(A) GTT, (B) AUC of GTT, (C) ITT, (D) AUC of ITT, (E) energy consumption of one mouse by weekly, (F) BW. n = 5, data were evaluated by Student's t-test.

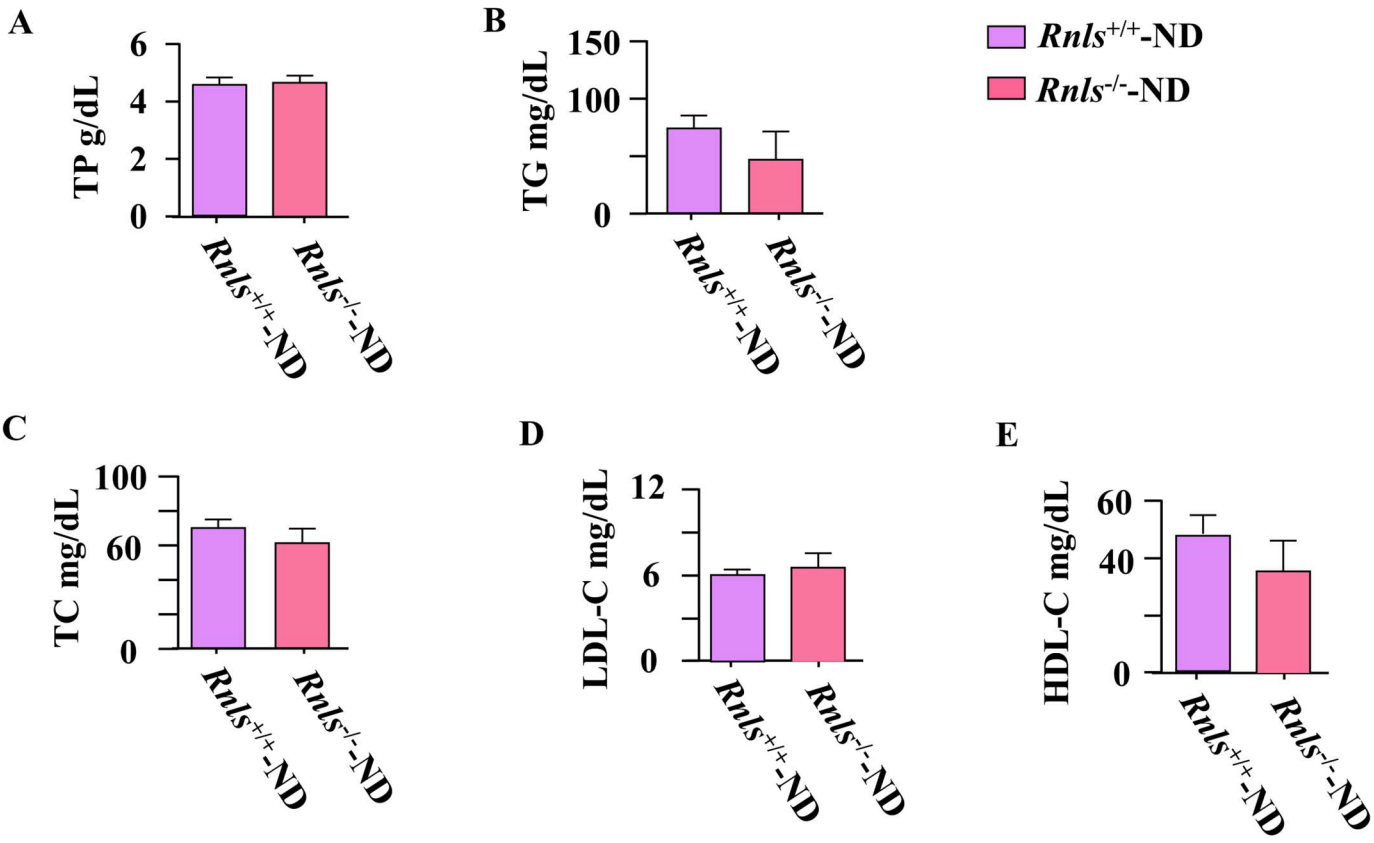


Figure 15. Plasma biochemical parameters of *Rnls*$^{-/-}$ and *Rnls*$^{+/+}$ mice under ND. (A) TP, (B)TG, (C) TC, (D) VDL-C, (E) HDL-C. n = 5, data were evaluated by Student's t-test.

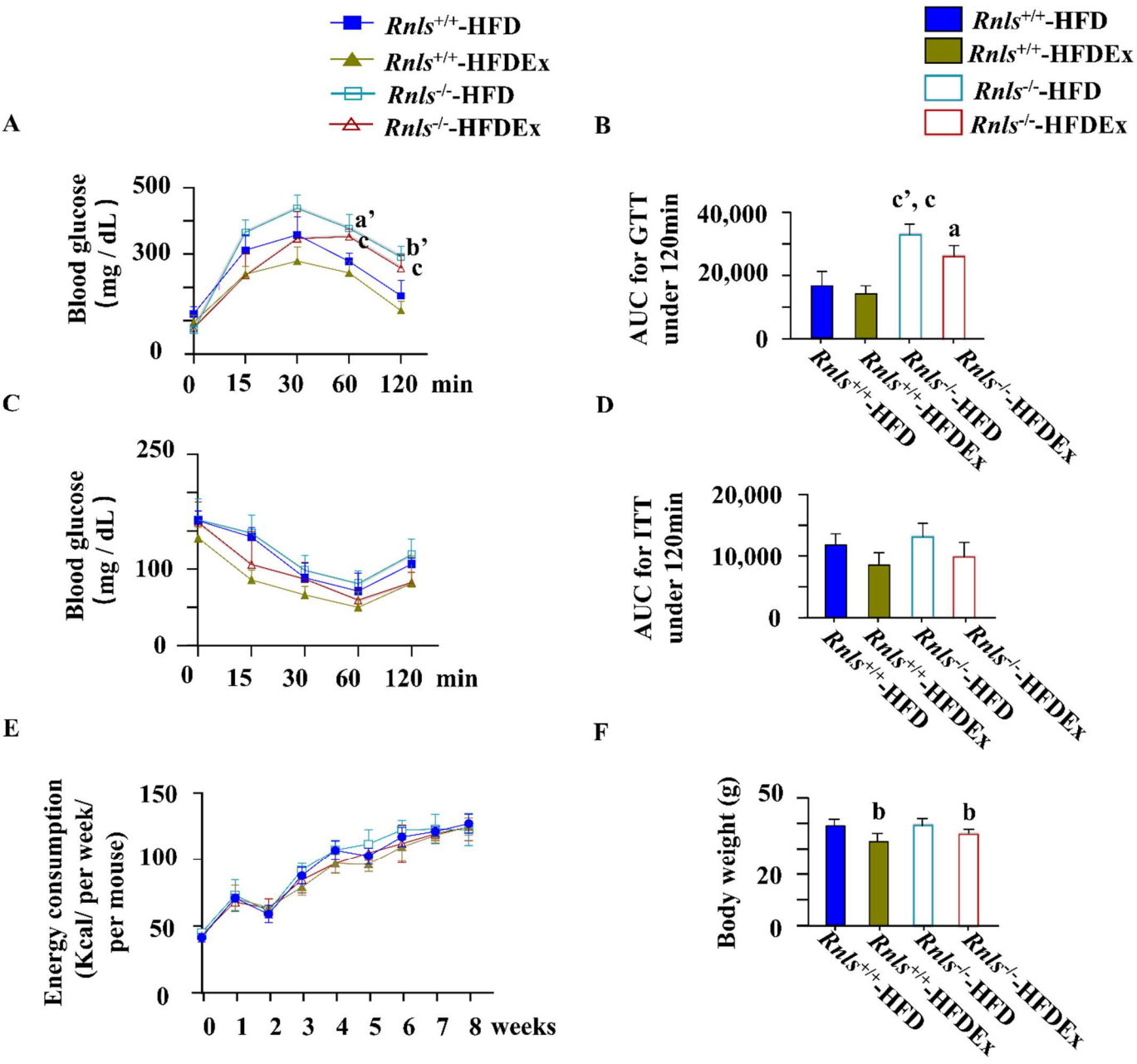


Figure 16. Phenotype of *Rnls*$^{-/-}$ and *Rnls*$^{+/+}$ mice with or without exercise intervention under HFD.

(A) GTT, (B) AUC for GTT, (C) ITT, (D) AUC for ITT, (E) energy consumption of one mouse by weekly, (F) BW. a', $p< 0.05$; b', $p<0.01$, c', $p<0.001$, compared to *Rnls*$^{+/+}$-HFD group. a, $p< 0.05$; b, $p<0.01$, c, $p<0.001$; compared to *Rnls*$^{+/+}$-HFDEx group. n = 5, data were evaluated by two-way ANOVA test.

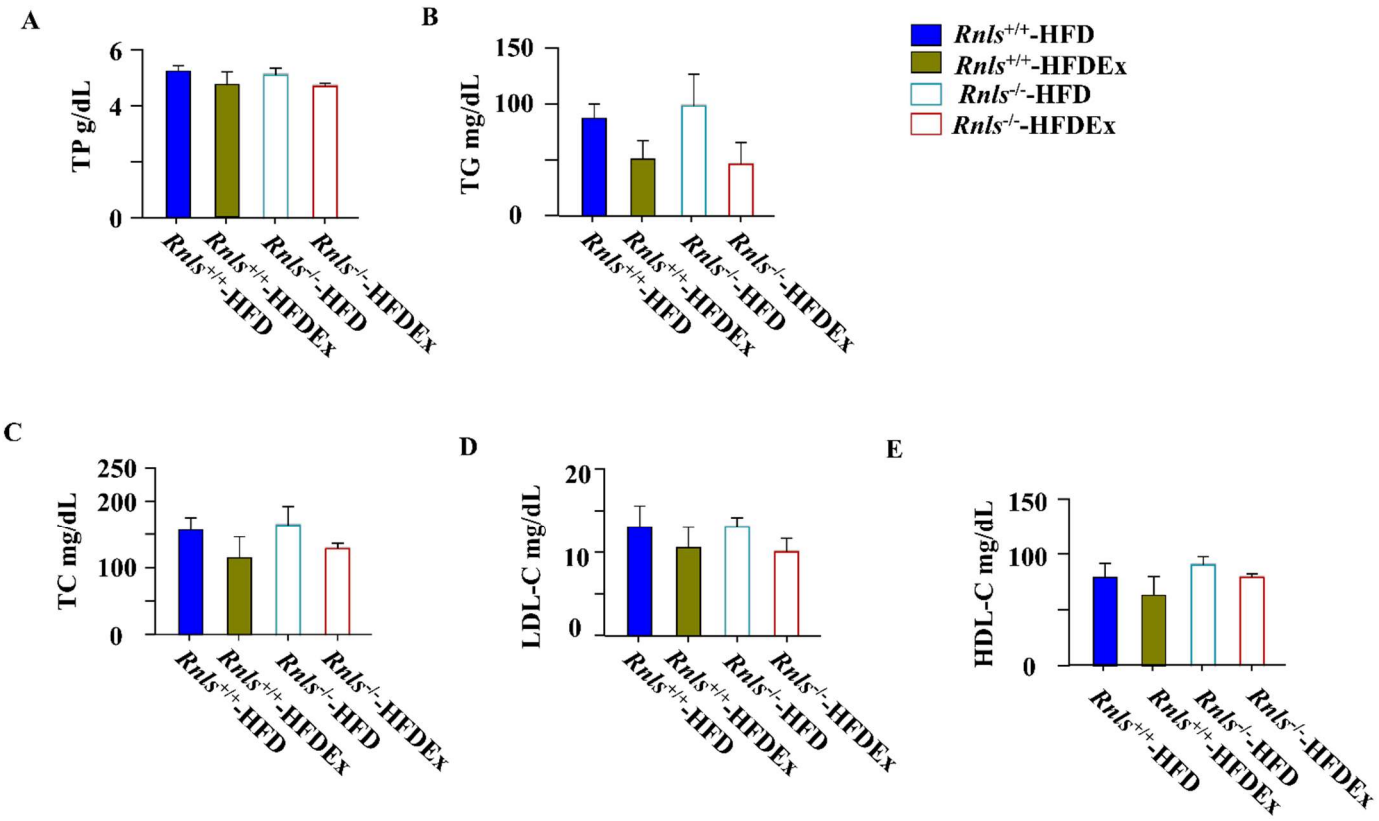


Figure 17. Plasma biochemical parameters of *Rnls*$^{-/-}$ and *Rnls*$^{+/+}$ mice with or without exercise intervention under HFD.

(A) TP, (B)TG, (C) TC, (D) VDL-C, (E) HDL-C. n = 5, data were evaluated by two-way ANOVA test.

# 4. Discussion

In order to explore the glucose tolerance in *Rnls*$^{+/+}$ and *Rnls*$^{-/-}$ mice under different interventions. Firstly, I analyzed the glucose tolerance of *Rnls*$^{+/+}$ and *Rnls*$^{-/-}$ mice under ND. My results showed that there was no difference of glucose tolerance by comparing BG level under ND. Then, to investigate the glucose tolerance of *Rnls*$^{+/+}$ and *Rnls*$^{-/-}$ mice under HFD with or without exercise, mice were fed with an eight -weeks continuous HFD with or without a treadmill training for four weeks. My findings revealed that there was not any different behavior of glucose tolerance by comparing BG level under HFD. Notably, exercise could not decrease the BG level of *Rnls*$^{-/-}$-HFD mice.

*Diet, exercise, and glucose tolerance*

As we all known, T2D is triggered by the following three main factors: genetic, diet, and exercise. among this, diet and exercise are easily to manage. The latest updates on diabetes management and treatment at the IDF Congress reported that diet and exercise are as the effective way to treat T2D. Some studies showed that high fiber diet could reduce body weight and BG level of T2D, while HFD induced BW increase and BG level [105, 106]. *Rnls*$^{+/+}$ and *Rnls*$^{-/-}$ mice has normal behavior on GTT under ND, moreover, there was no difference was exhibited in *Rnls*$^{+/+}$ and *Rnls*$^{-/-}$ mice at present study (Figure 14A and B). Hence, I wonder the behavior on GTT of *Rnls*$^{+/+}$ and *Rnls*$^{-/-}$ mice under HFD. Unsurprisingly, HFD impaired glucose tolerance of *Rnls*$^{+/+}$ and *Rnls*$^{-/-}$ mice, and it caused more severe situations for *Rnls*$^{-/-}$ mice (Figure 13A and B). Some previous studies showed that low to moderate density exercise are good for glucose level [107-110]. *Rnls*$^{+/+}$ mice was easily to alleviate glucose tolerance by four weeks treadmill training at current study (Figure 16A, B). However, four weeks treadmill could not alleviate the impaired glucose tolerance of *Rnls*$^{-/-}$ mice (Figure 16A, B). These results further identified that the importance of *Rnls* participates in glucose regulation with diet or exercise intervention.

*Diet, exercise and plasma biochemical parameters*

In this study, plasma biochemical parameters were well analyzed for evaluating the physiological and health status in clinical and disease animal models. Since that exercise protects against plasma biochemical parameters changes caused by HFD, several studies have observed these effects [111, 112]. Regrettably, we did not see difference in *Rnls*$^{+/+}$ and *Rnls*$^{-/-}$ mice under different interventions. It suggested *Rnls* seems not important for lipid metabolism.

*Renalse and exercise*

Bozena CP et.al demonstrated that the renalase protein reduction in white muscle influenced by exercise is related to blood redistribution in muscle [49]. One latest investigation showed that renalase expression was elevated by aerobic exercise training to improve renal injury in rat through increasing in medulla [50]. Various studies also revealed that acute or moderate and high intensity exercise are easily to increase renalase level in muscle and blood [46-48]. I used *Rnls* knockout mice to determine it function on exercise at present study. On the one hand, I found that *Rnls* knockout impaired exercise efforts to improve BG; on the other hand, I found that *Rnls* knockout seems no effect on exercise to improve plasma biochemical paremeters, especially for lipid metabolism.

# 5. Summary

Study 1 showed that BG level of *Rnls*$^{+/+}$ and *Rnls*$^{-/-}$ mice was no difference during IPGTT under ND. However, HFD caused *Rnls*$^{-/-}$ mice difficult to reduce its glucose level during IPGTT compared with *Rnls*$^{+/+}$ mice. What's more, this impaired glucose tolerance could not be rescued by exercise in *Rnls*$^{-/-}$ mice. This study confirmed that *Rnls* knockout is negative for glucose metabolism under HFD.

# V study 2

Exploring GM composition of *Rnls*$^{+/+}$ and *Rnls*$^{-/-}$ mice under ND or HFD.

## 1. Aim

This study hypothesized that GM composition of mice was remodeled by *Rnls* knockout not only diet intervention. The purpose of this study was to demonstrate how *Rnls* affects GM composition.

## 2. Material and methods

*Animals and experimental design*

B6;129S1-Rnlstm1Gvd/J mice were obtained from the Jackson Laboratory. Identification of wild-type (*Rnls*$^{+/+}$) and *Rnls* knockout (*Rnls*$^{-/-}$) mice was done using Polymerase Chain Reaction as described previously [104]. The animals were housed in a room at 12-h/12-h light-dark cycle conditions and the temperature was maintained at the range of 20°C–26°C.

After acclimatizing for 7 days *Rnls*$^{+/+}$ mice and *Rnls*$^{-/-}$ (10 each, male, 4-weeks-old) mice were divided into groups by randomization. They were grouped as follows: *Rnls*$^{+/+}$-HFD (n = 5), *Rnls*$^{-/-}$-HFD (n = 5), *Rnls*$^{+/+}$-ND (n = 5) and *Rnls*$^{-/-}$-ND (n = 5). HFD group mice were feed with a high-fat diet whereas ND group was given a normal diet like study 1. Table 1 shows the composition of fatty acids of HFD.

All protocols of this study were conducted according to the recommendations of animal work approved by the Animal Subjects Committee, University of Tsukuba, Japan (approval number: 21–027).

*Fecal DNA extraction*

Fecal DNA was extracted using the NucleoSpin DNA tool (U047A, Takara Bio, Tokyo, Japan) from the feces as described by manufacturer's protocol.

*16s rRNA sequencing*

16S ribosomal ribonucleic acid gene V3-V4 region was amplified using dual-indexed V3-V4 region primer using barcodes. Primer sequence is as follows;

314F 5′-TCGTCGGCAGCGTCAGATGTGTATAAGAGACAGCCTACGGGNGGCWGCAG-3′ and 806R 5′-GTCTCGTGGGCTCGGAGATGTGTATAAGAGACAGGGATACHVGGGTWTCTAAT-3′.

Amplification was done at AM-Pure XP. Illumina MiSeq was used to conduct the PE300 sequencing. Library quality was evaluated using Quant-iT dsDNA Assay Kit (Invitrogen). The Illumina MiSeq platform was used for library sequencing followed by the generation of the 300-bp paired-end reads. Sequencing of the 16S rRNA gene was conducted by Takara Bio, Japan. For generating taxon bins with a specific taxonomy, operational taxonomic units (OTUs) of identical taxonomic classification were pooled into one bin upon the threshold of 99% identity. The α- and β-diversity of microbial communities were analyzed using quantitative insights into microbial ecology 2 (QIIME2) [113-115]. For the determination of α-diversity Chao1, Shannon Diversity Index, observed species OTUs, and Faith's phylogenetic diversity (Faith-pd) were used. While β-diversity distances were measured using unweighted and weighted UniFrac to generate Principal Coordinate Analysis (PCoA) plots [116]. A heat map profile was generated using R (http://www.rproject.org/). To elucidate differences in bacterial taxa we used linear discriminant analysis (LDA) effect size (LEfSe). LEfSe algorithm with the Huttenhower Galaxy web application (The Huttenhower Lab, Boston, MA; http://huttenhower.sph.harvard.edu/lefse/) was used to plot the cladogram.

*Statistical analysis*

Data are presented as mean ± standard deviation. A two-way analysis of variance followed by Tukey's post hoc test was used for statistical analysis using GraphPad Prism 8.0.1 (GraphPad Software. Inc). The p-value of $<0.05$ was considered statistically significant.

Table 1. research diet (D12492).

| Fatty acids name | Contents | Fatty acids name | Contents | Fatty acids name | Contents | Fatty acids name | Contents |
|---|---|---|---|---|---|---|---|
| C10, Capric | 0.1 | C16:1, Palmitoleic | 3.4 | C18:3, Linolenic | 5.2 | C20:4, Arachidonic | 0.7 |
| C12, Lauric | 0.2 | C17 | 0.9 | C20, Arachidic | 0.4 | C22:5, Docospentaenoic | 0.2 |
| C14, Myristic | 2.8 | C18, Stearic | 26.9 | C20:1 | 1.5 | | |
| C15 | 0.2 | C18:1, Oleic | 86.6 | C20:2 | 2.0 | | |
| C16, Palmitic | 49.9 | C18:2, Linoleic | 73.1 | C20:3 | 0.3 | | |

Note: Fat and oil tests conducted in the fourth quarter of 2011 were used to generate the fatty acid profile. D12492 was prepared using Lard (245 grams) and Soybean oil as a sample (25 gram).

# 3. Results

*Intestinal microbial α diversity and β diversity*

To evaluate richness and evenness, first at all, observed OTUs were showed by sequencing depth (Figure 18A). After that, index of shannon, chao1 and faith-pd were displayed in Figure 15B to D. Besides, each group had their own clustering were well performed with unweighted PCoA (Figure 19A), while weighted PCoA verified the identical clustering to some extent (Figure 19B), regardless of the limited graphical evidence.

*Intestinal microbial composition at phylum and family level*

We performed 16srRNA sequencing to analyze the microbiota distribution differences among *Rnls*$^{+/+}$ *and Rnls*$^{-/-}$ mice groups. A total of 160 bacterial genera were observed among the four groups (Figure 18A), and each group maintained a unique microbiota. Venn diagram analysis revealed that 160 OTUs were common among all the groups while, 270, 290, 252, and 236 OTUs were unique to *Rnls*$^{+/+}$-ND, *Rnls*$^{-/-}$-ND, *Rnls*$^{+/+}$-HFD, and *Rnls*$^{-/-}$-HFD groups respectively (Figure 20A). We analyzed the abundance of microbiota at the phylum level to get the insights into microbiota composition of all the groups. An increased abundance of Firmicutes was observed in the mice group which received the HFD diet, along with a decrease in Bacteroidetes abundance (Figure 20B). We observed an increase in the abundance of Firmicutes accompanied by a decrease of Bacteroidetes in the *Rnls*$^{-/-}$-ND group as compared to the *Rnls*$^{+/+}$-ND group (Figure 20B). Moreover, we calculated the Firmicutes/Bacteroidetes ratio since it is related to obesity, and no difference was observed among the four groups (Figure 20B). Analysis at the family showed that HFD had an increased abundance of Clostridiales, Desulfovibrionaceae, [Paraprevotellaceae], and Ruminococcaceae, while a decreased abundance of Bifidobacteriaceae, Lactobacillaceae, and S24-7 as compared to the ND groups (Figure 20C). When analyzed individually we found that S24-7 and Lactobacillaceae have significantly higher levels in ND-fed mice groups as compared to HFD groups

irrespective of the mice genotype. Lachnospiraceae levels were unchanged throughout the groups, while [Paraprevotellaceae] abundance was higher in HFD groups as compared to ND groups. Notably, the ratio of Desulfovibrionaceae only increased significantly in the *Rnls*$^{+/+}$-HFD group (Figure 20C).

*Discovery representative bacteria at species level*

The Linear discriminant analysis Effect Size was used to analyze the species-level difference among the groups as shown in Figure 21. The most abundant species in the *Rnls*$^{+/+}$-ND group were *Bifidobacterium pseudolongum* (*B. pseudolongum*) and *Lactobacillus reuteri* (*L. reuteri*), whereas in *Rnls*$^{-/-}$-ND group abundance species belong to *Lactobacillus*, *Turicibacter*, and *S24-7* genera. Moreover, the *Rnls*$^{+/+}$-HFD group had a higher abundance of species belonging to *Mucispirillum, Prevotella,* and *Bacteroides* genera, while the *Rnls*$^{-/-}$-HFD group had *Anaerofustis Anaerotruncus*, *Parabacteroides*, and *Oscillospira* as representative species.

*Intestinal microbial heatmap of order level.*

A two-dimensional heatmap of the 20 most dominant orders was constructed to determine the pattern of the dominant microbial community influenced by *Rnls* and HFD (Figure 22). A hierarchical clustering based on the relative abundances of different orders could sufficiently differentiate between *Rnls*$^{+/+}$ from *Rnls*$^{-/-}$ mice. Both groups fed with ND diet had higher abundance of Lactobacillales. *Rnls*$^{+/+}$-ND group contained a higher abundance of Bifidobacteriales, Erysipelotrichales Rickettsiales, and Coriobacteriales, as compared to other groups, while, Anaeroplasma-tales, Burkholderiales, Bacteroidales, and Turicibacterales were increased in *Rnls*$^{-/-}$-ND group. Mice groups fed with an HFD diet had a higher abundance of Clostridiales. *Rnls*$^{+/+}$-HFD group presented an increase in Gemellales, Deferribacterales and Desulfovibrionales abundance, whereas, *Rnls*$^{-/-}$-HFD group had higher levels of RF39 and RF32. Altogether, our results suggest that distinct patterns of gut bacterial composition in *Rnls*$^{-/-}$ and *Rnls*$^{+/+}$ mice are influenced by the type of diet given to mice.

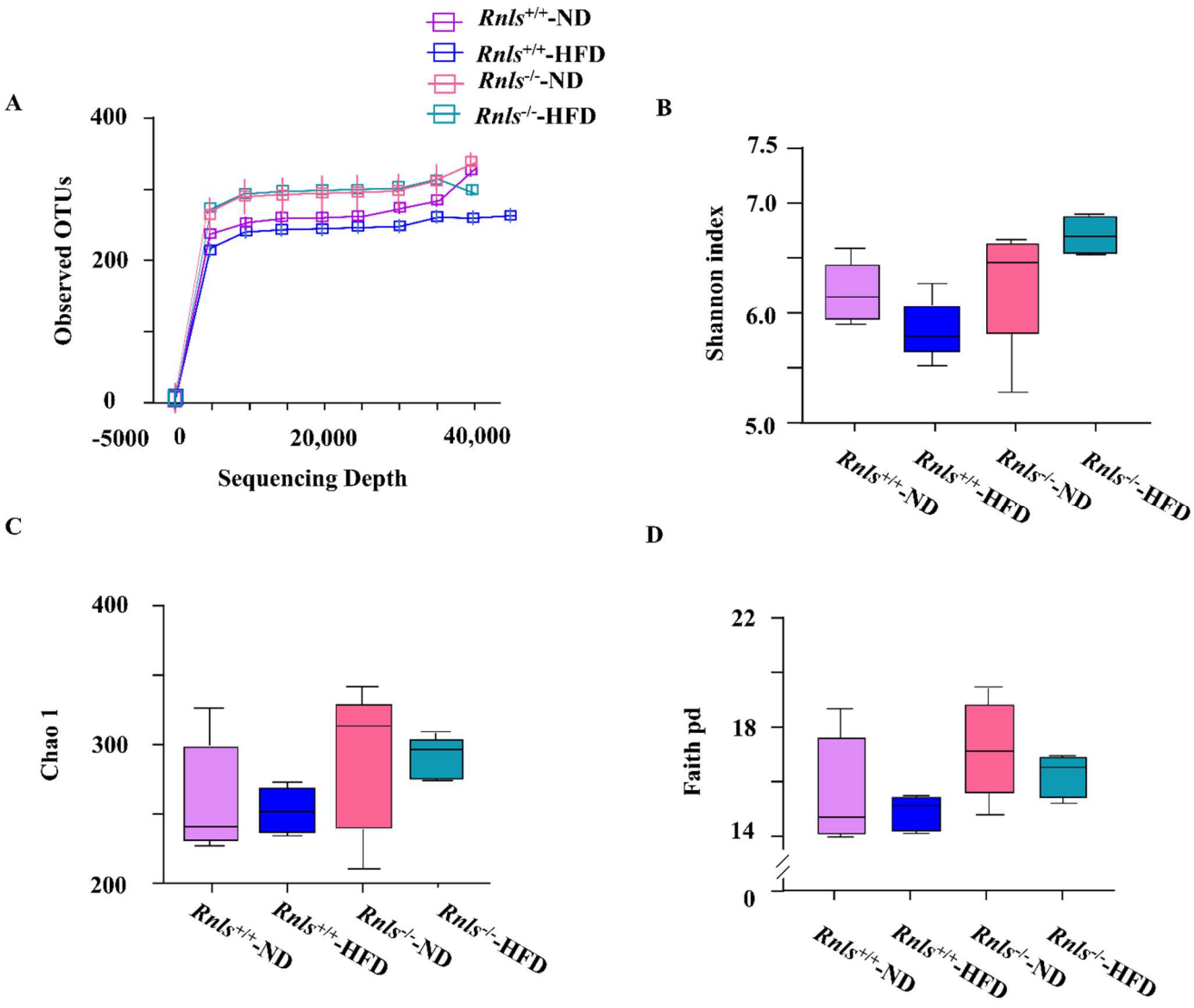


Figure 18. Intestinal microbial α-diversity.

(A) Observed OTUs, (B) Index of Shannon, (C) Index of Chao1, and (D) Index of Faith-pd. n = 5.

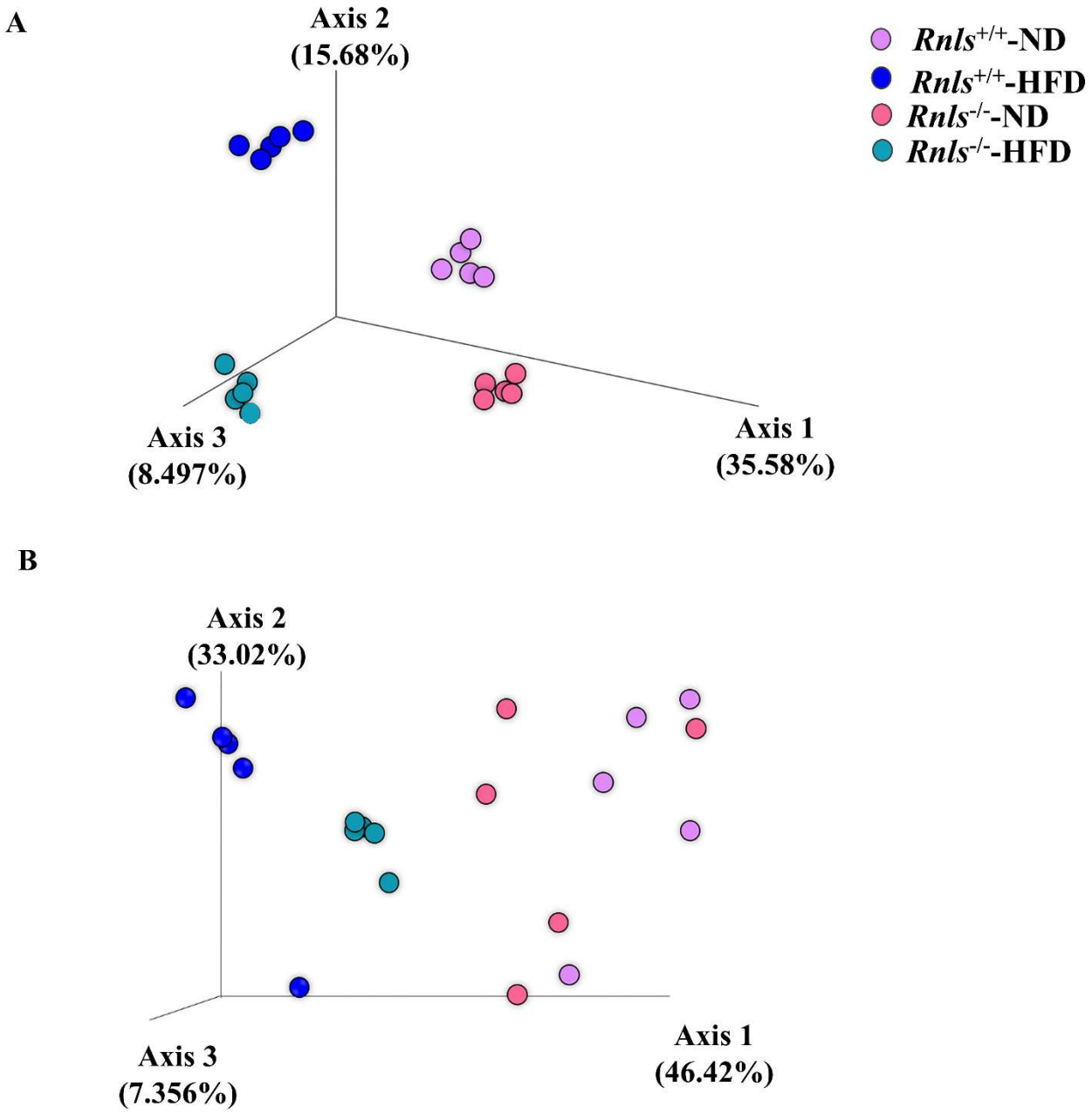


Figure 19. Intestinal microbial β diversity.

(A) unweighted UniFrac distance matrices (B) weighted UniFrac distance matrices n = 5.

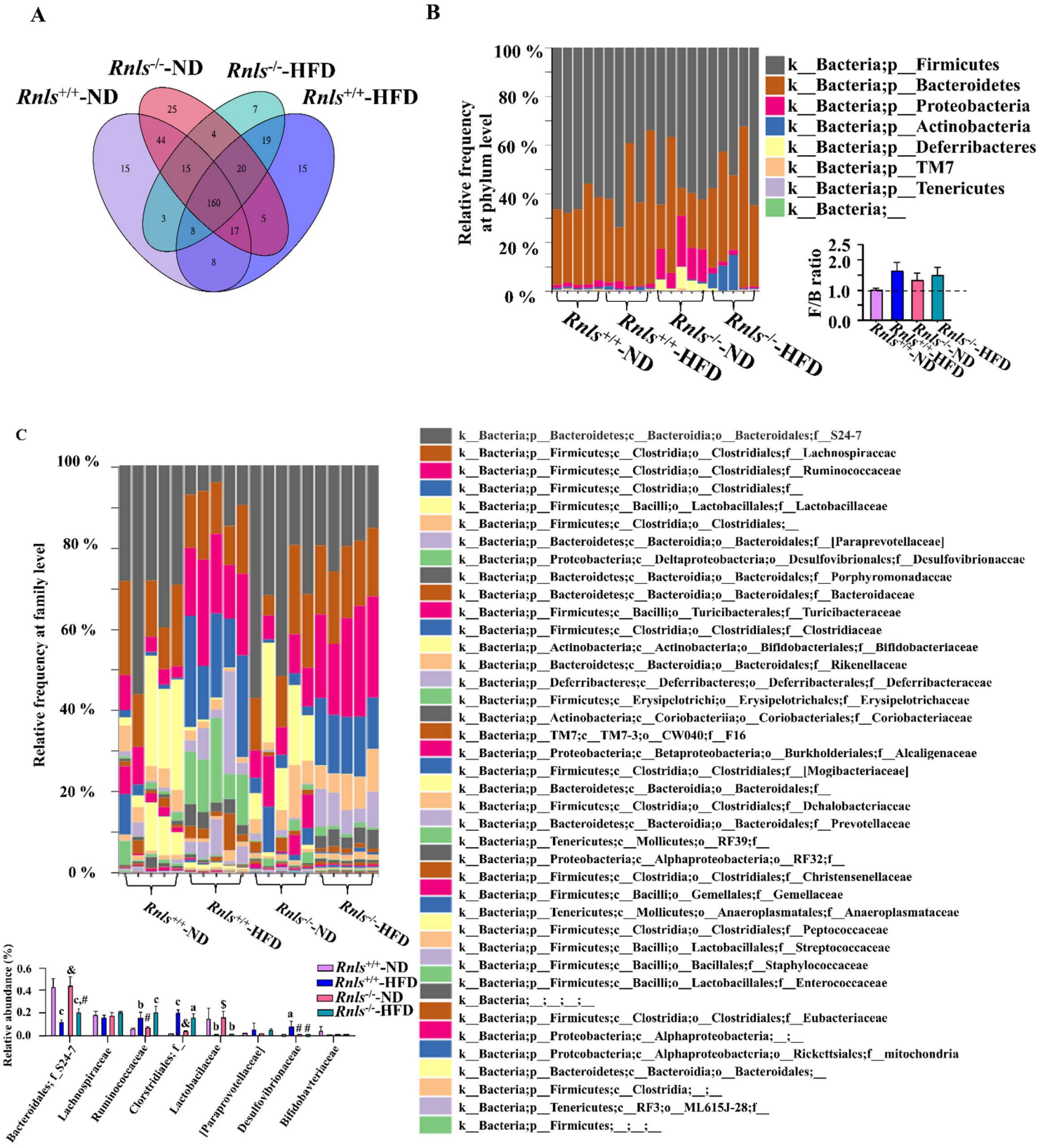


Figure 20. Intestinal microbial composition at phylum and family level.

(A) Venn, (B) Phylum level, (C) Family level, a: $p < 0.05$, b: $p < 0.01$, c: $p < 0.001$,

compared with the *Rnls*$^{+/+}$-ND group. #: $p < 0.05$, $: $p < 0.01$, &: $p < 0.001$, compared with the *Rnls*$^{+/+}$-HFD group. n = 5, data were evaluated by two-way ANOVA test.

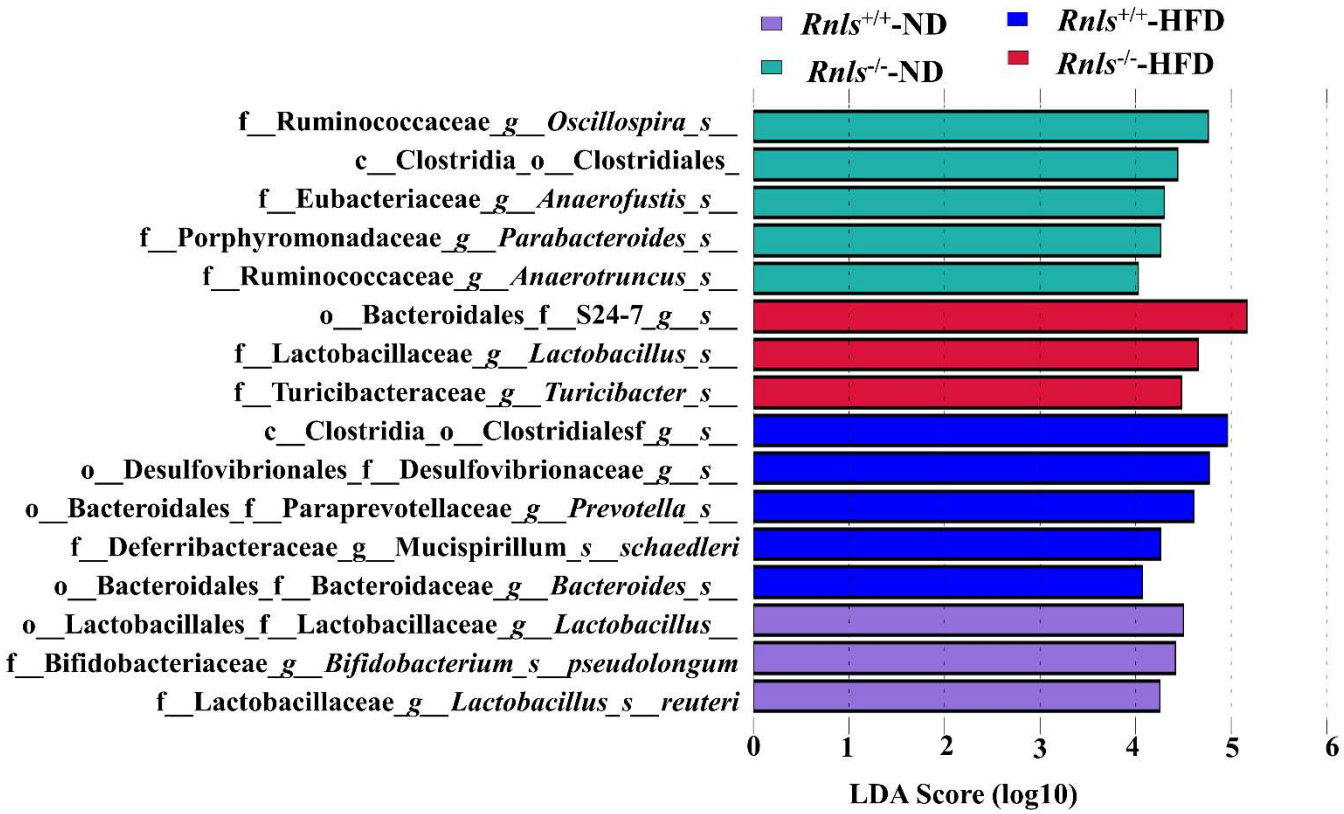


Figure 21. Discovery representative bacteria at species level. n = 5.

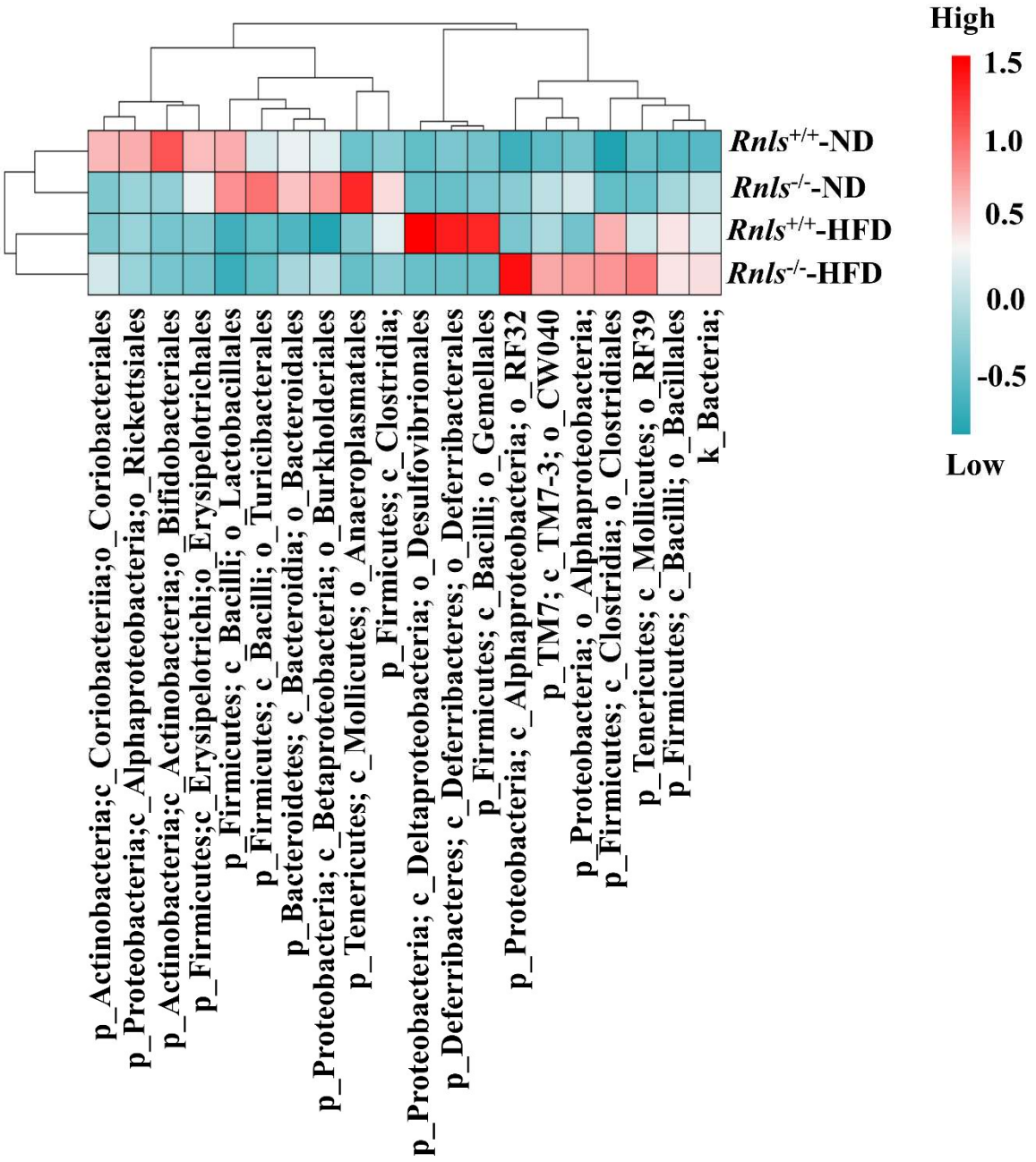


Figure 22. Intestinal microbial heatmap of order level. n = 5.

# 4. Discussion

In study 1 I have shown that *Rnls* knockout leads to impaired glucose regulation under HFD. Therefore, to explore the possible way for *Rnls* effect on glucose metabolism (in study 2), the reasons for the impaired glucose metabolism from the perspective of GM. The results showed that not only diet, but also *Rnls* knockout can regulate the Firmicutes/Bacteroidetes ratio, which promoted the GM dysbiosis under HFD. The reduction of *L. reuteri* and *B. pseudolongum*, as well as the growth of pathogenic bacteria, became one of the reasons for the impairment of glucose metabolism.

*Diet, microbiota and T2D*

Researchers have been concentrating on the GM as a crucial component of metabolism in recent years. Distribution of the microbiota is influenced by genotype, growth, and dietary habits, which is further connected to obesity, diabetes, and its comorbidities [88, 117]. Due to the tight connection between diabetes and the GM, the GM composition was thoroughly examined in my investigation. α diversity and β diversity were first contrasted. I have come to the conclusion that the four groups' samples all had appropriate sequencing depth and show various grouping patterns. (Figure 18 and 19). The GM composition was then assessed at several levels, including phylum, order, species, and so on. HFD altered the S24-7, Lactobacillaceae, Ruminococcaceae, and Clostridiales microbiota composition. (Figure 20). Additionally, the dysbiosis GM and obesity brought on by HFD are concomitant with the increased Firmicutes and decreased Bacteroidetes abundance. [118, 119]. *Rnls* knockout may accelerate the onset of obesity or diabetes by altering the ratios of Firmicutes and Bacteroidetes, which is surprising given that $Rnls^{-/-}$ mice also showed a large abundance of Firmicutes under ND conditions. In my investigation, the LDA score was applied to detect substantially different species among groups. (Figure 21). Both *L. reuteri* and *B. pseudolongum*, which have been referred to as probiotics in earlier investigations, were significantly different in the $Rnls^{+/+}$-ND group [120-122]. In the $Rnls^{-/-}$-ND group, *S24-7* and *Lactobacillus* were very different, and they had been

linked to a reduction in the risk of obesity [123]. Additionally, I discovered that several bacteria, (Figure 19), such as *Prevotella*, *Bacteroides*, Desulfovibrionaceae, *Anaerotruncus*, and *Turicibacter* [67, 124], are connected to T2D and obesity in the $Rnls^{+/+}$-HFD, $Rnls^{-/-}$-ND and $Rnls^{-/-}$-HFD group. *Anaerotruncus* and Desulfovibrionaceae were found in greater numbers in human hypercholesteremia patients [125]. Due to the increased abundance of these harmful bacteria, even though *Oscillospira* and *Parabacteroides* appeared in $Rnls^{-/-}$-HFD group, and they are advantageous to glucose metabolic and lipid metabolic pathways, although their numbers of detrimental bacteria have risen [126], but did not still perform in a manner comparable to *L. reuteri* and *B. pseudolongum* of the $Rnls^{+/+}$-ND group. My findings are in line with earlier research, showing that while genetic inheritance influences the emergence and configuration of the GM, there are variances between bacterial populations even if some bacterial populations serve the same purpose. [22, 68]. My findings implied that *Rnls* knockout could have an impact on the GM diversity and composition. The top 20 orders of species were also shown on a heatmap to assess the dominating species among the four groups. In the $Rnls^{+/+}$-ND group, Lactobacillales and Bifidobacteriales bacteria predominated, whereas Lactobacillales and Anaeroplasmatales bacteria dominated in the $Rnls^{-/-}$-ND group. In the HFD group, Clostridiales predominated among the microorganisms (Figure 22). Overall, as earlier research have revealed, *Rnls* and the bacteria associated to *Rnls* may be potential options in the early detection and prevention of diabetes [34, 43].

# 5. Summary

Our study shows that *Rnls* knockout leads to intestinal microbiota dysbiosis. At the phylum level, we observed an increase in the abundance of Firmicutes while a decrease in Bacteroidetes abundance was witnessed. Moreover, we found that *Rnls* effects the microbial genera depending on the diet feed to the mice. Since in ND groups *Turicibacter* and *Lactobacillus* were in abundance while, in HFD groups *Anaerotruncus, Parabacteroides,* and *Oscillospira* were abundant. Glucose intolerance phenomena was

exhibited by the *Rnls*$^{-/-}$ mice in comparison to *Rnls*$^{+/+}$ mice when given an HFD diet. Taken together our results suggest that *Rnls* knockout may escalate the dysbiosis of gut microbiota leading to an increased risk of metabolic diseases.

# VI Study 3

Illustrating the metabolites from GM to regulate the function of enteroendocrine L cells.

## 1.Aim

This study hypothesized that metabolites of microbiota can activate endocrine L cell to exert their function on glucose metabolism. Therefore, metabolites of gut microbiota were extracted from feces to illustrate the influence on endocrine L cells. STC-1 cell line was used in this study to imitate L cell bioactivity in vitro and explored the differences on cell proliferation and cell signaling pathway.

## 2. Material and methods

*Mice and Experimental design*

Jackson Laboratory (CA, USA) provides Fifteen healthy male B6,129S1-Rnlstm1Gvd/J mice (*Rnls*$^{-/-}$ mice, four weeks old) and C57BL/6J mice (wild-type mice (*Rnls*$^{+/+}$); four weeks old) were obtained from. Five mice were kept in one microisolator cage, which had a temperature range 23–26 ℃ and a humidity level of 60%. Also included was a 12-h light/dark cycle and unlimited access toward a ND and sterile water. The mice were separated into *Rnls*$^{-/-}$-ND (n = 15) and *Rnls*$^{+/+}$-ND (n = 15) groups after acclimating for one week and mice in each group were numbered from one to fifteen, fed with ND throughout the experimental period (8 weeks). Throughout the entire process of using animals in experiments, adhering to the University of Tsukuba's Animal Care Committee's rules (permission number: 21-027).

*Fecal supernatant preparation*

Thirty clean and sterile microisolator cages were taken without bedding substrate and numbered the cage according to the grouping of mice. Afterwards, each group’s

mice were put in correspondingly numbered cages (one mouse per cage) and allowed to defecate naturally. After 5-10 minutes, 3-5 droppings were visible in each cage. The feces were then picked up with sterile forceps and placed in two pre-labelled 10 ml centrifuge tubes (marked as *Rnls*$^{+/+}$-ND and *Rnls*$^{-/-}$-ND group). Samples of fresh feces from *Rnls*$^{+/+}$-ND and *Rnls*$^{-/-}$-ND groups (1 g from each group) were collected and each mouse contributed. After that, dissolved in 5 mL phosphate buffer (PBS: 10 mmol/L $Na_2HPO_4$, 1.76 mmol/L $KH_2PO_4$, 137 mmol/L NaCl and 2.7 mmol/L KCl) and homogenized on ice. Subsequently, the homogenized solution was centrifuged (10000 ×g, 10 min, 4℃) as described in earlier research [127, 128]. Supernatants were collected, and coarse particles and bacteria were removed by filtration using a 0.22-μm filter (Millex-GV, Merck Millipore Limited, Tullagreen, Ireland.) [127, 128]. Figure 23 depicted the concrete details.

*Cell culture*

STC-1 cell line was purchased from American Type Culture Collection (CRL-3254™, ATCC, VA, USA). Cell culture was performed in Dulbecco's modified Eagle's medium (Cat#11965092, DMEM; high glucose with L-glutamine; Thermo Fisher Scientific, MA, USA) with 100 mg/mL streptomycin, 100 U/mL penicillin, and 10% fetal bovine serum (Cat#CCP-FBS-BR-500, FBS; Cosmo Bio, Tokyo, Japan). Cells were grown at 37 ℃ and 5% $CO_2$.

*Cell viability assay*

$1.5 \times 10^5$ cells/well were seeded into 12-well plates, which were then treated with 50 μL fecal supernatant (from *Rnls*$^{+/+}$ and *Rnls*$^{-/-}$ mice) or 50 μL PBS plus 2% FBS DMEM (1.15 mL) after overnight culture in DMEM. The resazurin assay was used to determine cell viability as previously described . Briefly, after 48 h of treatment, each well was placed medium (1 mL) containing 0.004% resazurin (Cat#R0203, Tokyo Chemical Industry, Tokyo, Japan) and kept for 3 h at 37 ℃. Subsequently, a 96-well black plate was used for holding medium (100 μL) from each well. The medium's fluorescence intensity was detected at 590 nm emission and 569 nm excitation

wavelengths using Varioskan LUX (Thermo Fisher Scientific, MA, USA). All treatments were performed three times each.

*Western blotting*

6-well plates were used for seeding 5 × $10^5$ cells/well. After that, at 85%–90% confluence, the culture medium was changed to 2% FBS DMEM. STC-1 cells were stimulated with 100 μL fecal supernatant or 100 μL PBS plus 2% FBS DMEM (2.3 mL). After 48 h of treatment, collected cells for analyzing RNA and protein. All treatments were performed in triplicates.

Cells were scraped from plates into ice-cold NP40 lysis buffer (1% NP40, 50 mmol/L Tris-HCl, pH 7.5; 150 mmol/L NaCl,) that containing a protease inhibitor cocktail (Cat#25955-24, Nacalai Tesque, Kyoto, Japan) and phosphate inhibitor (Cat#4906845001, Roche, Basel, Switzerland) tablets in a microtube. After centrifuging the protein lysates at 12,000 × g for 15 min at 4℃, the supernatants were moved to fresh microtubes after centrifuged. Subsequently, a BCA assay kit (Cat#T9300A, Takara Bio, Tokyo, Japan) was used to detect protein concentrations according to the guidance from manufacturer. The protein lysate (2 mg/mL) were adjusted with 2× loading buffer containing 2-mercaptoethanol before being denatured at 95 ℃ for five minutes. Afterward, at 120 V for 90 minutes, sodium dodecyl sulfate-polyacrylamide gel electrophoresis (10%) was performed for separation the prepared sample. Subsequently, a polyvinylidene fluoride membrane was used for proteins transmembrane by an overnight wet transfer method at 25 V, 4℃. TBS-T buffer (0.05% Tween 20, 150 mmol/L NaCl, 50 mmol/L Tris-HCl, pH 7.6) including 5% skim milk was used for blocking the membrane for 60 minutes before washing three times (5 minutes each time, TBS-T buffer). The membrane was treated with the primary antibody specified in Table 1 overnight at 4℃ with gentle shaking. The membrane was washed with TBS-T buffer three times (5 minutes each time) the next day before being treated with the secondary antibody: anti-rabbit IgG (1:5000, #7074, Cell Signaling Technology, MA, USA) and anti-mouse IgG (1:5000, #7076, Cell Signaling Technology, MA, USA) at room temperature for 60 minutes with gentle shaking. After

three washes with TBS-T buffer, the target protein bands were seen on FUSION FX7.EDGE (Vilber Lourmat, Marne-la-Vallee, France) with a chemiluminescence reagent (WSE-7120, EzWestLumi Plus, ATTO, Tokyo, Japan) and saved as TIFF images. Finally, using ImageJ Fiji (version Java 8, Bethesda, USA) to quantify the intensity of the bands.

*Gene expression analysis*

STC-1 cells were grown and harvested as indicated in the preceding section. Afterward, using Sepasol-RNA I Super G (Cat#09379-55, Nacalai Tesque, Kyoto, Japan) to extracting RNA under the guidance from manufacturer. The expression of *Pc1/3* in STC-1 cells stimulated with distinct fecal supernatants was quantified well. Milli-Q water was used to fix the content of extracted total RNA to 100 ng/μL. cDNAs were generated using the PrimeScript RT Master Mix (Cat#RR036A, Takara Bio, Tokyo, Japan) under the guidance from manufacturer. For the quantitative polymerase chain reaction (qPCR), cDNAs were diluted into 10 times by MilliQ water firstly. The qPCR reaction volume comprised 5 μL master mix (Cat#RR820S, TB green Premix Eaq II, Takara Bio, Tokyo, Japan), 2.8 μL Milli-Q water, 0.1 μL primer solution (10 μmol/L forward and reverse each), and 2 μL template. The amplification was monitored using the QuantStudio 5 Real-Time PCR System (Thermo Fisher Scientific, MA, USA). Thermal cycling conditions described in the following: one cycle (95℃/5 min), subsequently 40 cycles (95℃/3 s), and melting curve analysis (60℃/30 s). Table 3 displayed the primer. All qPCR tests were performed three times. Relative gene expression was normalized by GAPDH, and analyzed it using quantification cycle (Cq) values and the two delta-delta CT ($2^{-\Delta\Delta CT}$) method.

*Analysis of the enzymatic hydrolysis activity of Boc-Arg-Val-Arg-Arg-MCA*

To evaluate the enzymatic hydrolysis activity of t-Butyloxycarbonyl-L-arginyl-L-valyl-L-arginyl-L-arginine 4-methylcoumaryl-7- amide (Boc-Arg-Val-Arg-Arg-MCA), 12-well plates were used to seed ($1.5 \times 10^5$ cells/well) STC-1 cells. At 85%–90% confluence, 2% FBS DMEM was used as culture medium. STC-1 cells were stimulated

with 50 μL mice fecal supernatant or 50 μL PBS plus 2% FBS DMEM (1.15 mL). All treatments were performed in triplicates. Co-cultured cells at 0, 6, 12, 24, 36, 48h were scraped from plates into ice-cold NP40 lysis buffer (1% NP40, 50 mmol/L Tris-HCl (pH 7.5), 150 mmol/L NaCl,) containing a protease inhibitor cocktail (Cat#25955-24, Nacalai Tesque, Kyoto, Japan) and phosphate inhibitor (Cat#4906845001, Roche, Basel, Switzerland) tablets in a microtube. After centrifuging the protein lysates at 12,000 × g for 15 minutes at 4°C, the supernatants were moved to fresh microtubes. Subsequently, using a BCA assay kit (Cat#T9300A, Takara Bio, Tokyo, Japan) to detect the protein concentrations following the guidance from manufacturer. Fixing protein lysate to 3 mg/mL for further study.

The Pc1/3 proteinase is the mammalian equivalent of the KEX2 proteinase, while KEX2 included other processing endopeptidases, such as Pc2, Pc4, Pc4 and so on. Some protein or peptide precursors have been shown to be correctly converted into mature forms by encoded enzymic cleaving of mostly after basic amino acid couplings such as Lys-Arg and Arg-Arg. Hence, using the peptide (Boc-Arg-Val-Arg-Arg -MCA, 3155-V, Peptide Institute Inc, Osaka, Japan) to analyzing the enzyme activity. Fifteen microgram (5 μL) protein lysates as the enzyme source were added to the assay buffer (5 μL, 4 mmol/L Boc-Arg-Val-Arg-Arg-MCA and 40 μL, 0.1% bovine serum albumin-1mmol/L $CaCl_2$). After 30 minutes at 37°C, and the mixture reaction was terminated by 200 μL, 1 mol/L acetic acid. Finally, measuring fluorescence intensity with emission 460 nm/excitation 380 nm [129]. One unit (1U) of enzyme activity was described as following defined as the fluorescence intensity increased per 0.01 into the appropriate product after 30 minutes at 37°C.

*Analyzation the total GLP-1 level*

Total GLP-1 ELISA Kit was bought from Yanaihara Institute Inc (YK161), Tokyo, Japan. The whole protocol was seriously carried on. The secretion of GLP-1 from culture medium (n=3) were detected in this study.

*Statistics*

GraphPad Prism version 8 software (GraphPad Software, CA, USA) was used to

do one-way analysis of variance (ANOVA) with Tukey's test to compare the variations among the three groups, and an unpaired t-test to compare the variations between the two groups. For displaying data, using the mean ± standard deviation. Statistically significant was defined as P values of $< 0.05$.

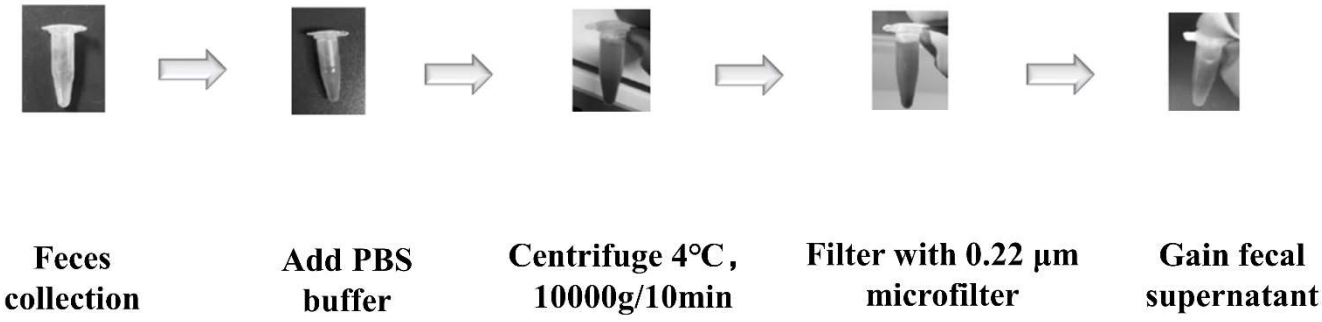


Figure 23. Fecal supernatant extraction.

Table 2. Antibody dilution and manufacturer

| Antibody name | Company and code | Dilution |
|---|---|---|
| p44/42 | Cell signaling technology, #4695 | 1:1000 |
| p-p44/42 | Cell signaling technology, #4377 | 1:1000 |
| SAPK/JNK | Cell signaling technology, #9252 | 1:1000 |
| p-SAPK/JNK | Cell signaling technology, #4668 | 1:1000 |
| AKT | Cell signaling technology, #9272 | 1:1000 |
| p-AKT | Cell signaling technology, #9271 | 1:1000 |
| GAPDH | Santacruz Biotechnology, sc-365062 | 1:1000 |

Table 3. Primer sequences of GAPDH and Pc1/3.

| Gene name | Primer sequence | |
|---|---|---|
| Pc1/3 | Forward primer | 5’-GCEAAGAGGCAGTTTGTTAATGA-3’ |
| | Reverse primer | 5’-TGATTTCAAGTGATCCAATCTG-3’ |
| GAPDH | Forward primer | 5'-GGAAACCCATCACCATCTTC-3' |
| | Reverse primer | 5'-GTGGTTCACACCCATCACAA-3' |

# 3. Results

*Fecal supernatant from Rnls$^{+/+}$ mice effectively promotes the cell proliferation of STC-1 cell line*

Figure 24. displayed that STC-1 cells co-cultured with fecal supernatants for 48 h proliferated more than those co-cultured with PBS (*Rnls*$^{+/+}$-ND group vs. PBS group, $P < 0.01$; *Rnls*$^{-/-}$-ND group vs. PBS group, $P < 0.05$).

*Fecal supernatant from Rnls$^{+/+}$ mice effectively activated the Akt/JNK signaling pathway in STC-1 cells*

To further elucidate the role of metabolites in L cell activation, we incubated fecal supernatant with STC-1 cells and analyzed the classic signaling pathway, such as phosphorylation level of P44/42 (p-P44/42), SAPK/JNK (p-SAPK/JNK), and AKT (p-AKT). STC-1 cells co-cultured with the fecal supernatant from *Rnls*$^{+/+}$ mice had high expression of p-SAPK/JNK and p-AKT relative to that of GAPDH (Figure 25A and B). However, there was no difference in p-P44/42 expression among the three groups (Figure 25B). In addition, the ratio of p-AKT/AKT, p-P44/42/P44/42, and p-SAPK/JNK/SAPK/JNK demonstrated similar results (Figure 25C-E). STC-1 cells co-cultured with the fecal supernatant from *Rnls*$^{+/+}$ mice showed an increased p-AKT/AKT and p-SAPK/JNK/SAPK/JNK ratio, while there was no difference in p-P44/42/P44/42.

*Fecal supernatant from Rnls$^{+/+}$ mice elevates the Pc1/3 mRNA expression in STC-1 cell line*

Quantification of the mRNA expression of Pc1/3 demonstrated that STC-1 cells co-cultured with the fecal supernatant from *Rnls*$^{+/+}$ mice showed elevated mRNA expression of Pc1/3 compared to those co-cultured with fecal supernatant from *Rnls*$^{-/-}$ mice and PBS. STC-1 cells co-cultured with the fecal supernatant from *Rnls*$^{-/-}$ mice did not influence the mRNA expression of Pc1/3 (Figure 26).

*The fecal supernatant enhanced the enzymatic hydrolysis activity of Boc-Arg-Val-Arg-*

*Arg-MCA of STC-1 cells with a time-dependent manner.*

To understand the impacts of fecal supernatant on the enzymatic hydrolysis activity of Boc-Arg-Val-Arg-Arg-MCA of STC-1 cells, I monitored the changes in the enzymatic hydrolysis activity of Boc-Arg-Val-Arg-Arg-MCA over time. my findings demonstrated that the enzymatic hydrolysis activity of Boc-Arg-Val-Arg-Arg-MCA performed time-dependent, increasing from 0 to 12 h and decreasing after that till 48 h, and it reached the peak in each group at 12 h (Figure 27A and B). This result suggested that the enzymatic hydrolysis activity of Boc-Arg-Val-Arg-Arg-MCA seemed like unrelated to *Rnls*$^{+/+}$ or *Rnls*$^{-/-}$ mice's fecal supernatant. Moreover, the enzymatic hydrolysis activity of Boc-Arg-Val-Arg-Arg-MCA showed the highest in STC-1 cells stimulated with fecal supernatant from *Rnls*$^{+/+}$ mice (Figure 27C).

*The level of total GLP-1 secretion in STC-1 cells after stimulation with fecal supernatant was no difference*

To understand GLP-1secretion from L cells by fecal supernatant stimulation, I analyzed the concentration of GLP-1 in the culture medium (Figure 28), there was no difference between the fecal supernatant from *Rnls*$^{+/+}$ and *Rnls*$^{-/-}$ mice.

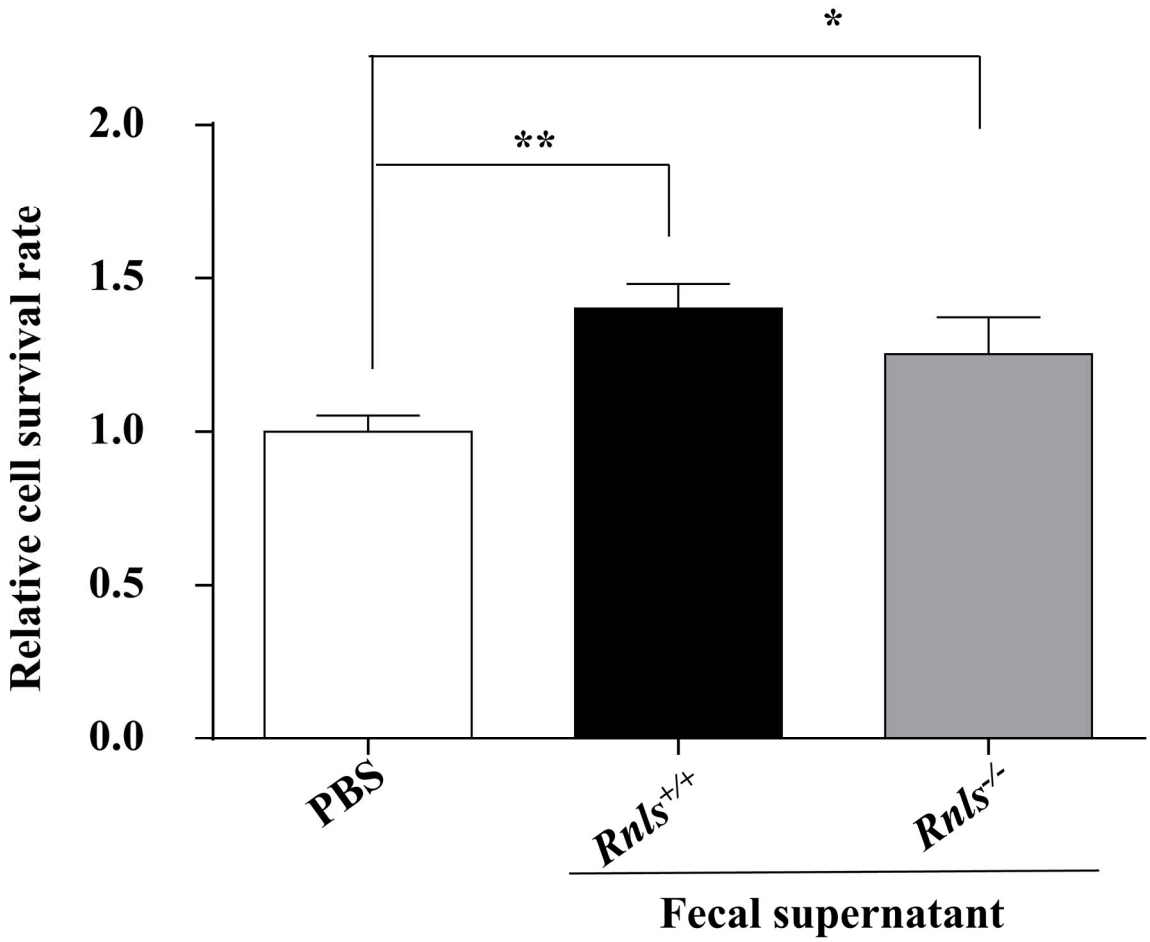


Figure 24. Effects of fecal supernatants from *Rnls*$^{+/+}$ and *Rnls*$^{-/-}$ mice on cell proliferation of STC-1 cell lines.

Relative cell survival rate. Treating STC-1 cells with fecal supernatants for 48 h. Asterisks indicate significant differences (*P < 0.05, **P < 0.01 vs. PBS). Data are described as the mean ± standard deviation (SD); evaluated by one-way ANOVA test. n = 3 in each group.

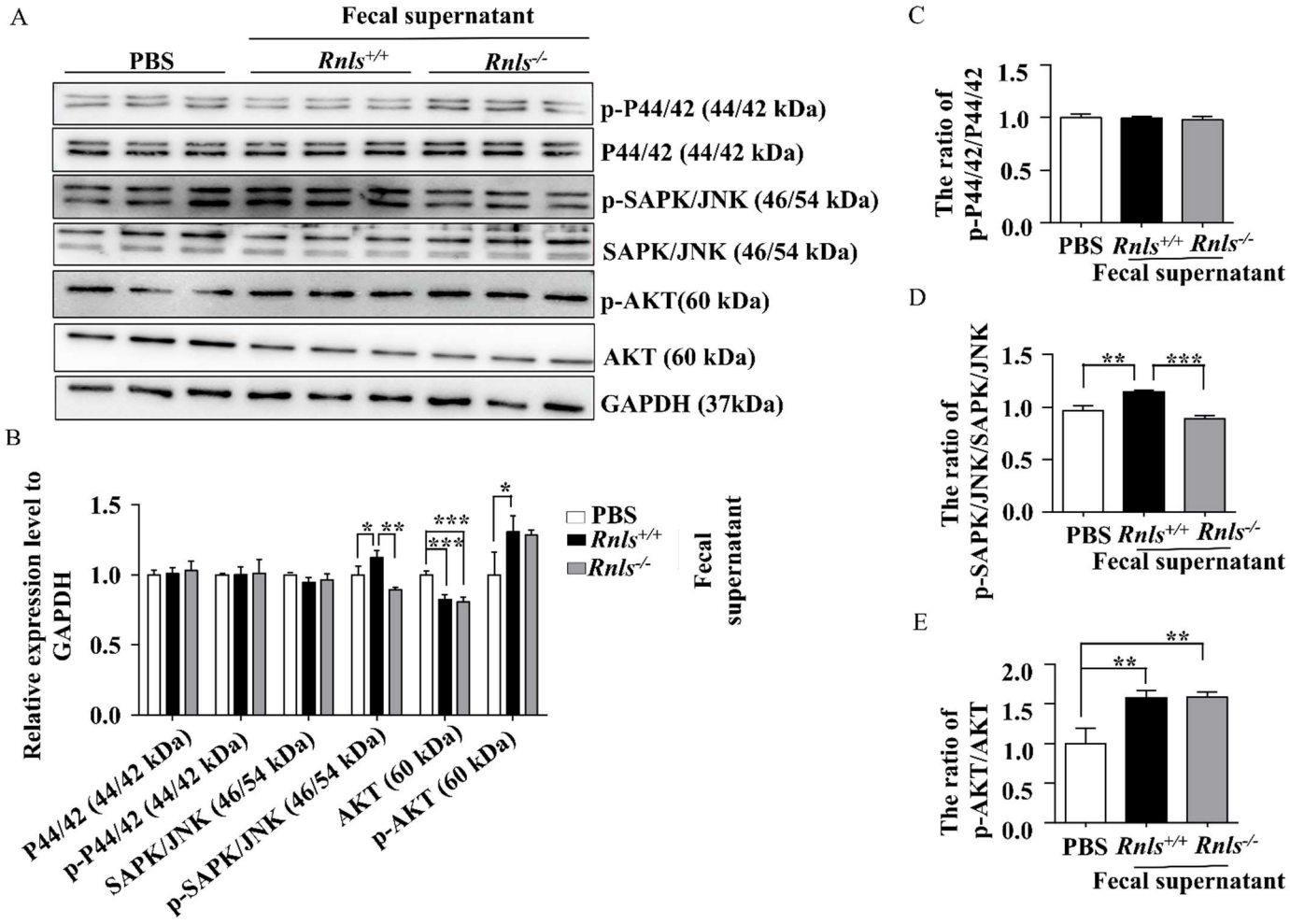


Figure 25. Effects of fecal supernatant from *Rnls*$^{+/+}$ and *Rnls*$^{-/-}$ mice on Akt/JNK signaling pathway activation in STC-1 cell lines.

The levels of p-P44/42, P44/42, p-AKT, AKT, p-SAPK/JNK, and SAPK/JNK, were analyzed using western blotting after stimulating STC-1 cells with different fecal supernatants for 48 h. (A) Western blot images, (B) The protein expression of p-P44/42, P44/42, p-SAPK/JNK, SAPK/JNK, p-AKT and AKT relative to GAPDH, the proportion of (C) p-P44/42/P44/42, (D) p-SAPK/JNK/ SAPK/JNK, and (E) p-AKT/AKT. *P < 0.05, **P < 0.01, ***P < 0.001 vs. PBS. Data are shown as the mean ± standard deviation; evaluated by one-way ANOVA test. n = 3 in each group.

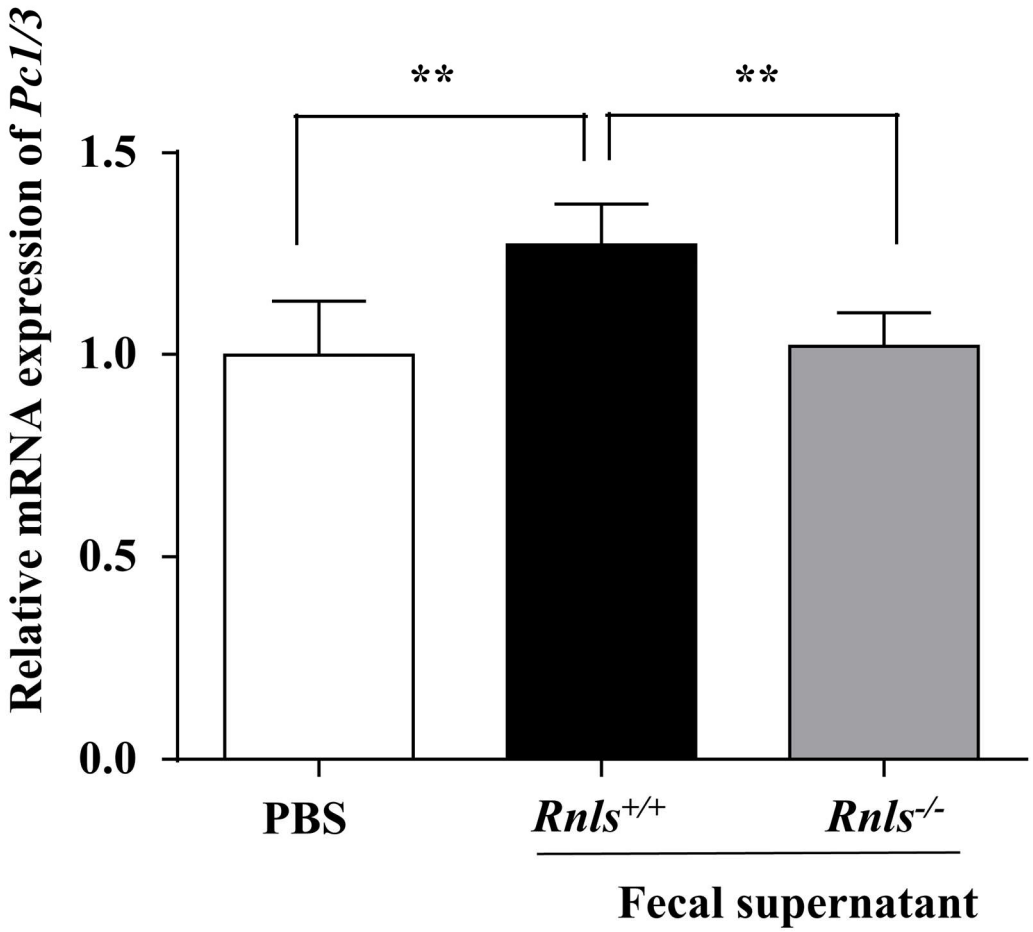


Figure 26. Effects of fecal supernatants from *Rnls*$^{+/+}$ and *Rnls*$^{-/-}$ mice on the *Pc1/3* mRNA expression in STC-1 cell lines.

After 48 h stimulating of STC-1 cells with different fecal supernatants, and using qPCR to detect the *Pc1/3* mRNA expression. **P < 0.01 vs. PBS. Data are displayed as the mean ± SD; evaluated by one-way ANOVA test. n = 3 in each group.

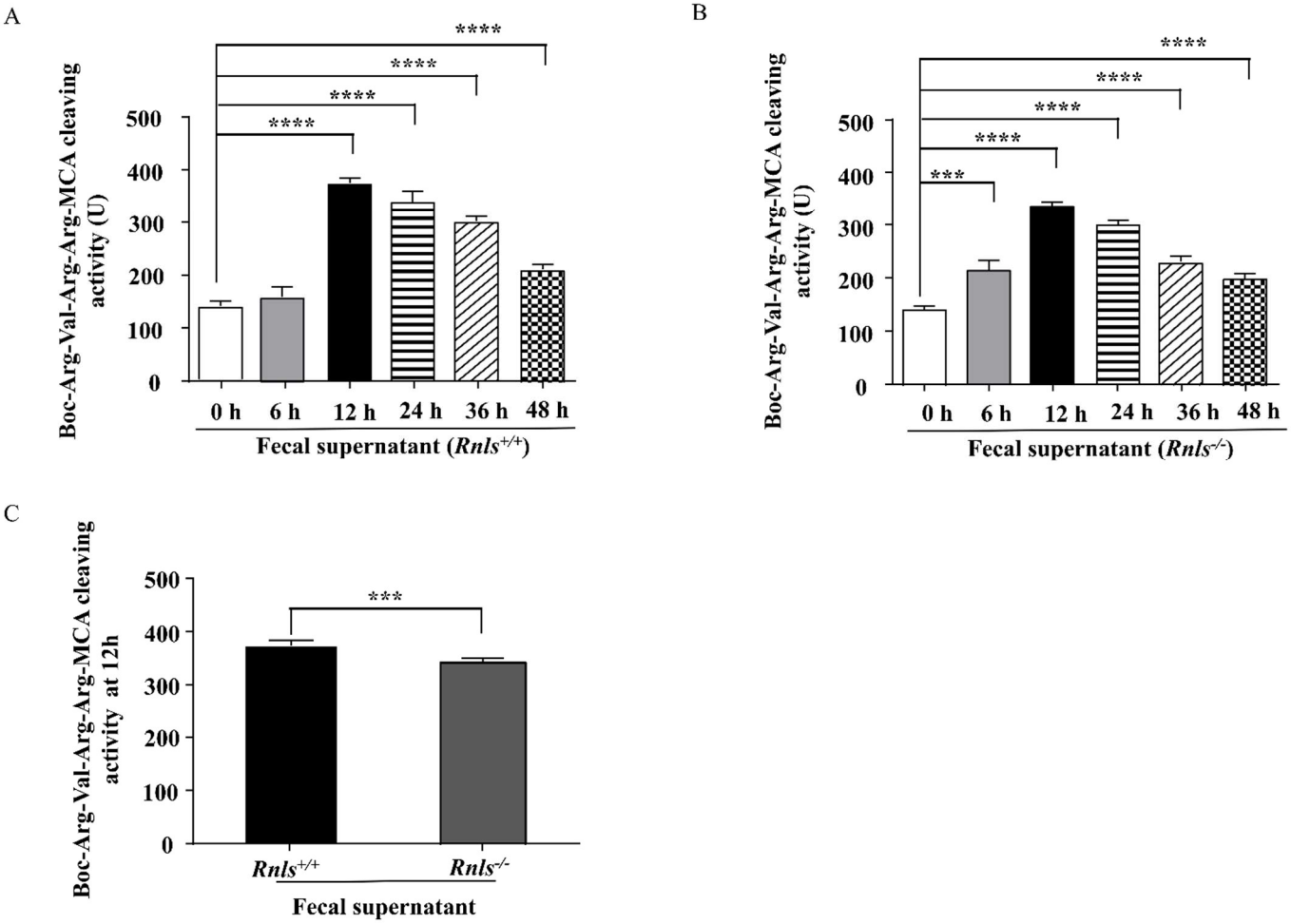


Figure 27. Effects of fecal supernatants from *Rnls*$^{+/+}$ and *Rnls*$^{-/-}$ mice on the enzymatic hydrolysis activity of Boc-Arg-Val-Arg-Arg-MCA of STC-1 cell line.

The enzymatic hydrolysis activity of Boc-Arg-Val-Arg-Arg-MCA of STC-1 cells co-cultured with fecal supernatants from *Rnls*$^{+/+}$ (A) and *Rnls*$^{-/-}$ (B) mice exhibited a time-dependent behavior. (C) The enzymatic hydrolysis activity of Boc-Arg-Val-Arg-Arg-MCA of STC-1 cells after 12 h co-culturing with different fecal supernatant. (A, B) ****P < 0.0001 vs. 0 h; Data are displayed as mean ± SD; evaluated by one-way ANOVA test n = 3 in each group. (C) *P < 0.05 vs. supernatant from *Rnls*$^{+/+}$ mice; Data are displayed as mean ± SD; evaluated by student-t test. n = 3 in each group.

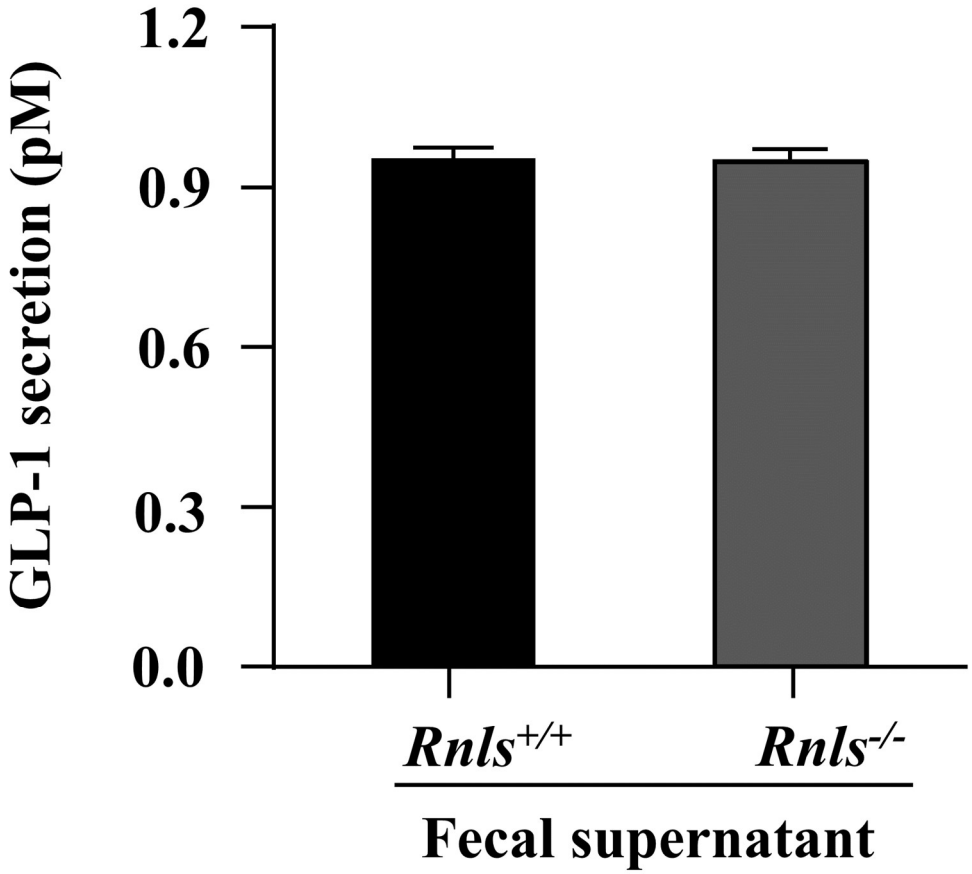


Figure 28. Concentration of total GLP-1 in STC-1 cells line at 12h.

Cells were cocultured with fecal supernatant stimulation from *Rnls*$^{+/+}$ and *Rnls*$^{-/-}$ mice. Data are displayed as mean ± SD; evaluated by student-t test. n = 3 in each group.

# 4. Discussion

In study 1 and 2, I clarified that *Rnls* knockout impaired glucose tolerance and imbalanced microbiota of mice. The underlying mechanism can be explained by study 3. In this study, the different metabolites of GM from $Rnls^{+/+}$ and $Rnls^{-/-}$ mice induced different endocrine L cell functions was demonstrated. Owing to *Rnls* knockout, metabolites from GM were changed, affected L cells proliferation and the expression and activity of Pc1/3. Then, influencing glucose metabolism.

*Gut homeostasis and the function of endocrine L cells*

Gut homeostasis is considered a key factor in maintaining endocrine L cell function and is influenced by the environment and host genetics [16, 75, 76]. Study 2 illustrated that *Rnls* plays a critical part in remodeling GM. The elevated Firmicutes/Bacteroidetes proportion and decreased *Bifidobacterium pseudolongum* abundance in $Rnls^{-/-}$ mice indicate raising risk of T2D [130], glycolipid dysfunction [131, 132]. Moreover, earlier research by our lab demonstrated that *Rnls* knockout accelerates the progression of nonalcoholic steatohepatitis; conversely, increased *Rnls* expression effectively decreased oxidative injury in Caco-2 cells [51, 104]. These results supported the protective properties of *Rnls*. In this study, I co-cultured STC-1 cells with the extracted fecal supernatant with abundant metabolites of microbiota from $Rnls^{+/+}$ and $Rnls^{-/-}$ mice. Comparing to PBS group, fecal supernatant from $Rnls^{+/+}$ mice elevated STC-1 cell proliferation more strongly after 48 h of co-culture, although there was also a substantial difference was observed in $Rnls^{-/-}$ fecal supernatant and PBS group. This result suggested that *Rnls* plays the critical part in cell proliferation, possibly through remodeling GM and their metabolites.

*Metabolites and cell signaling pathway*

SCFAs, secondary bile acids, and serotonin or 5-HT are examples of metabolites from GM, have been shown to influence glucose homeostasis [133-136]. Moreover, SCFAs and secondary bile acids also act on MAPK, Toll-like receptors, and Wnt and

play different roles in cell growth, inflammation, and aging [137, 138]. Reportedly, AKT/JNK signaling activation positively affects cell proliferation and metabolism [139-141]. Comparing with PBS group, fecal supernatants from *Rnls*$^{+/+}$ mice could effectively activate p-AKT no matter normalized to GAPDH or AKT, while there was only a significant difference of p-AKT was observed between *Rnls*$^{-/-}$fecal supernatant group and PBS group normalized to AKT. Moreover, fecal supernatant from *Rnls*$^{+/+}$ mice exhibited higher expression of p-SAPK/JNK in comparation with fecal supernatant from *Rnls*$^{-/-}$ mice group and PBS group. This finding suggested that *Rnls*$^{-/-}$ altered the microbiota-derived metabolites in the fecal supernatant, which led to the inactivation of p-Akt and p-SAPK/JNK enzymes and consequently lowered cell proliferation. In addition, several studies have demonstrated that *Rnls*, as a messenger, participates in acute injury and cancer progression [52, 142-144]. With the consideration of these, our results suggest a novel character of *Rnls* in the maintenance of cellular homeostasis.

*Metabolites and Pc1/3*

Metabolites from GM not only regulate cell growth but also participate in cell function. It has been shown that different performance in the GM modify the Pc1/3expression in mice fed a high fat diet [145]. Moreover, *Akkermansia muciniphila* proportion is associated with L cells's secretory capacity [77]. The metabolites from *Bifidobacterium* and *Lactobacillus* have been identified that maintaining glucose homeostasis by elevating several gut hormones levels through different signaling pathways [146-148]. Furthermore, study 2 demonstrated a decreased abundance of *Bifidobacterium* and *Lactobacillus* in *Rnls*$^{-/-}$ mice. Therefore, I speculated that the changes in microbiota composition and metabolites by *Rnls* knockout could affect the expression of Pc1/3. Concordant with this hypothesis, our results demonstrated that fecal supernatant from *Rnls*$^{+/+}$ mice increased the mRNA expression of *Pc1/3*. Furthermore, the enzymatic hydrolysis activity of Boc-Arg-Val-Arg-Arg-MCA, one crucial factor affecting its function [149], peaked after 12 h of fecal supernatant stimulation, and the fecal supernatants from *Rnls*$^{+/+}$ mice had a stronger effect on the

increased the enzymatic hydrolysis activity of Boc-Arg-Val-Arg-Arg-MCA than fecal supernatants from *Rnls*$^{-/-}$ mice.

*GLP-1 secretion*

The glucagon gene encodes a glucagon polypeptide (PG) consisting of 160 amino acids, of which positions 72 to 108 are sheared to form GLP-1. That is, GLP-1 is a small sequence encoded by the glucagon (GCG) gene. Prohormone convertase in intestinal L cells shears proglucagon to its carboxy-terminal peptide chain sequence, GLP-1. In study 3, in addition to testing the activity of Pc1/3, I also tested the secretion of GLP-1. However, unfortunately. We did not see a difference in GLP-1 secretion. I think this can be explained by 2 points: 1) The possible presence of Dipeptidyl Peptidase 4 (DPP4) enzyme in the cell culture medium. Previous research has suggested DPP4 is most vast in the intestine, and that the presence of DPP4 degrades GLP-1 and renders it inactive. The expression of DPP4 by STC-1 cells is not excluded here. 2) This experimental clock measured the quantity of total GLP-1 was not activated GLP-1. Although *Rnls*$^{+/+}$ mice had higher enzymatic hydrolysis activity of Boc-Arg-Val-Arg-Arg-MCA than that of *Rnls*$^{-/-}$ mice at 12h in study 3, *Rnls*$^{-/-}$ mice did not have a complete loss of enzyme activity and could also be cleaved efficiently. As the total GLP-1 levels measured here, there may be no difference. In addition, more research is necessary to discover if there is a difference in processing after Pc1/3 cleavage, the amount of active GLP-1. This is because earlier studies have shown that GLP-1(1-37) only has proinsulin secretory activity when the first six amino acids are cut off at the N-terminal end to become GLP-1(7-37).

# 5. Summary

In summary, our study showed that *Rnls* knockout impairs the *Pc1/3* mRNA expression and enzymatic hydrolysis activity of Boc-Arg-Val-Arg-Arg-MCA activity, which may accelerate glucose dysfunction progression thorough remodeling GM and their metabolites.

# VII Whole discussion

## 1. New knowledge

The following were the main conclusions of my thesis: i) *Rnls* knockout impaired glucose tolerance under HFD, and exercise could not improve glucose tolerance, ii) *Rnls* knockout led to intestinal microbial disruption in mice, especially, controlled *Oscillospira*, *Parabacteroides*, and *Anaerotruncus* under HFD, whereas *Lactobacillus* and *Turicibacter* were under ND. iii) *Rnls* knockout impairs the *Pc1/3* mRNA expression and enzymatic hydrolysis activity of Boc-Arg-Val-Arg-Arg-MCA by regulating GM and its metabolites, which may accelerate glucose dysfunction progression.

Aiming to demonstrate the importance of *Rnls* during exercise-enhanced glucose tolerance through GM diversity. The single nucleotide polymorphism of *Rnls* can accelerate the progression of T2D. However, the regulated function of *Rnls* involves in the development of T2D is still unclear. In experiment 1, to demonstrate the impact of *Rnls* knockout on BG level under different intervention conditions. First at all, four weeks old male $Rnls^{-/-}$ mice and wild type $Rnls^{+/+}$ mice were fed ND for eight weeks. Finally, analyzing the possibly different behavior in blood glucose tolerance. The results confirmed that compared with $Rnls^{+/+}$ mice, there was no distinction in BW, serum biochemical indexes, and glucose tolerance test of $Rnls^{-/-}$ mice under ND. It can be concluded that *Rnls* knockout does not adversely affect blood glucose level with ND. Next, in order to reveal whether *Rnls* knockout affects blood glucose level on HFD and whether exercise improves blood glucose level of *Rnls* knockout mice with HFD. Four-week-old male $Rnls^{-/-}$ mice and $Rnls^{+/+}$ mice were separated to 4 groups at random: $Rnls^{-/-}$-HFD, $Rnls^{+/+}$-HFD, $Rnls^{-/-}$-HFDEx, $Rnls^{+/+}$-HFDEx. A high fat diet was applied for the whole experimental period (eight weeks), while exercise group was given a moderate intensity treadmill training (20m/min, 5days/per week) from the fourth week of the experimental period. The results confirmed that, compared with $Rnls^{+/+}$ mice, the $Rnls^{-/-}$ mice exhibited no difference in body weight and serum biochemical indicators

with the HFD, while showed a higher glucose level during the glucose tolerance test. More importantly, the *Rnls*$^{-/-}$ mice still showed a higher glucose level with exercise intervention compared with *Rnls*$^{+/+}$ mice. It can be concluded that *Rnls* knockout has a negative impact on blood glucose level under HFD, and exercise could not alleviate such a negative impact.

GM and its metabolites are involved in the BG regulation were revealed recently. In experiment 2, in order to explore the reason why *Rnls* knockout performed differences in blood glucose level between ND and HFD, I next performed gut microbiota analysis. Results demonstrated that the abundance of *Bifidobacterium* in the gut microbiota of *Rnls*$^{-/-}$ mice was reduced under ND compared with *Rnls*$^{+/+}$ mice. Moreover, GM of *Rnls*$^{-/-}$ mice was imbalanced under HFD, and pathogenic bacteria increased. Thus, *Rnls* knockout changed GM composition. Previous study described that certain bacteria (e.g. *Bifidobacterium*, *Akkermansia*, *Lactobacillus*) and their metabolites can effectively stimulate the hormones secretion from intestinal endocrine L cells by influence on its cell proliferation and the *Pc1/3* mRNA expression, which promotes insulin release to regulate BG level. In study 3, to demonstrate the effect of GM composition changes on regulating the function of enteroendocrine L cells, I first extracted the fecal supernatant of *Rnls*$^{-/-}$ mice and *Rnls*$^{+/+}$ mice under a normal diet. Meanwhile, STC-1 cells line was selected to perform in vitro stimulation experiments. The fecal supernatants of mice were added to STC-1 cells separately, and their proliferation and *Pc1/3* mRNA levels were monitored. The results showed that the fecal supernatant from *Rnls*$^{+/+}$ mice on a normal diet could more effectively promote the proliferation of STC-1 cells, and the mRNA expression and enzyme activity of Pc1/3 were both at higher levels. Although the fecal supernatant of *Rnls*$^{-/-}$ mice could enhance STC-1 cells proliferation to some extent, it failed to increase the *Pc1/3* mRNA expression, even though it remained the enzymatic hydrolysis activity of Boc-Arg-Val-Arg-Arg-MCA partly. It can be confirmed that the *Rnls* knockout affects the function of enteroendocrine L cells by changing the metabolites of gut microbiota.

## 2. Limitation and perspective

Although I clarified *Rnls* knockout could regulate glucose metabolism by remodeling gut microbiota, some limitations existed in this thesis.

First, in study 1, eight weeks HFD failed to cause insulin resistance of $Rnls^{-/-}$ mice and $Rnls^{+/+}$ mice although induced obesity and glucose intolerance. As for the reason, could be explained by some earlier research [150, 151]. On the one hand, insulin resistance varies between species of mice; one the other hand, insulin resistance would like to be formed in various animal models by long term (over eight weeks) HFD or HFD plus high glucose. As we all known, insulin resistance is another obvious behavior for the development of T2D. Exercise had the ability to alleviate changed plasma biochemical parameters induced by HFD was illustrated in previous studies [111, 112]. However, I failed to get the similar result in my study. It is possible to explain by the following reasons: 1) circadian rhythm of exercise [152, 153]; 2) exercise intensity [154]; 3) exercise period [155], 4) continuous HFD [156]. In the future study, more strict experimental design should be made to avoid these limitations.

Second, I only proposed a possible way of *Rnls* to participate the process of glucose metabolism by GM, however, the exact interaction among exercise, gut microbiota and *Rnls* still need more focus on. Research to date has shown that acute exercise, moderate to high intensity exercise, increases renalase levels and gene expression in muscle and blood [46, 48-50]. Moreover, high-intensity exercise increased renalase level in mice on a high-fat diet [46]. Notably, exercise has the ability to regulate the homeostasis of gut microbiota, and germ-free mice had a terrible behavior in muscle mass and sports ability. Besides, in some previous studies, HFD caused the dysbiosis of GM while exercise could alleviate the dysbiosis of GM [83, 84]. All of them suggested a close relationship among GM, *Rnls* and exercise. Study 1 and 2, *Rnls* knockout contributes to the dysbiosis of GM and glucose intolerance under HFD. The reduction of *L. reuteri* and *B. pseudolongum*, as well as the growth of pathogenic bacteria, became one of the consequences for the impaired glucose metabolism. Additionally, exercise could not alleviate the impaired glucose tolerance of $Rnls^{-/-}$ mice

under HFD. It indicated that *Rnls* is important for exercise-enhanced glucose tolerance. What's more, previous studies revealed that increased renalase level and gene expression in muscle is related to acute exercise and moderate intensity exercise [46-49]. It means *Rnls* plays somewhat role in energy homeostasis. It is a pity that I did not analyze the GM composition of mice under HFDEx. In the future, I would like to reveal the GM composition and metabolites of mice under HFDEx. To reveal the exact role of *Rnls* in exercise-enhanced glucose tolerance by comparing the difference of GM composition and metabolites.

Last, fecal supernatant was extracted, and I demonstrated that *Rnls* knockout caused the changes of metabolites, then impaired the endocrine L cells' function by Akt/JNK pathway. Metabolites of fecal supernatant did not identify in study 3 because of technique limitation. Though these metabolites can be identified by LC-MS, separating personally and molecular structure analysis are still difficult. As we all known, there are numerous metabolites of GM, including SCFAs, bile acids, 5-HT, and so on. The amount of these will cause different changes in cell signaling pathways [37, 38, 157]. In the future, metabolic pathway analysis should be performed to reveal the exact metabolites species and involved cell signaling pathway.

Since the discovery of renalase in 2005, research on it has never stopped. First it was thought to be a specific type of monoamine oxidase that broke down catecholamines to lower blood pressure. As research progressed, its multi-tissue distribution and genetic polymorphisms were explored in relation to health. Through my PhD thesis, the possible pathways that renalase plays in the development of T2D were revealed. In the future, we can use renalase as a biomarker for the diagnosis of T2D and detect its levels from blood and urine by means of biochemical analysis. Genomic analysis will also be performed to analyze the renalase gene typing and gut microbiota composition. To prepare for future precision medical care in the clinical treatment process. In brief, on the one hand, specific strains of renalase gene associated bacteria can be developed to enhance L cells proliferation and the *Pc1/3* mRNA expression and enzymatic hydrolysis activity of Boc-Arg-Val-Arg-Arg-MCA in diabetic patients through fecal transplantation or oral capsules of the strains, thereby

increasing insulin secretion and improving blood glucose. On the other hand, gene editing techniques can be used to modify the transcriptional process of renalase gene and thus correct protein expression to treat diabetes. In recent years, it has been shown that renal aminase can act as a cytokine to activate cellular signaling pathways in the host, promoting cell proliferation and antioxidant and anti-inflammatory effects. The development of renalase receptor activators is then imperative. Previous studies have shown that renalase level was elevated after exercise; and, as a result of my PhD thesis, renalase gene knockout attenuates the effects of exercise. This illustrates the importance of renalase for the maintenance of the effects of exercise. Therefore, in the future, renalase supplements could be developed to counteract post-exercise fatigue and to achieve anti-acidification and anti-inflammatory effects.

# VIII Conclusion

Taken together, this study revealed the pathway by which *Rnls* participates in blood glucose regulation by remodeling GM, and the *Rnls* is neccesary for exercise-enhanced glucose tolerance.

# IX Acknowledgments

First at all, I want to convey my heartfelt appreciation to Prof. Takekoshi K, whose unwavering encouragement and insightful remarks were vital during my PhD studies. Prof. Takekoshi K, Prof. Watanabe K, Prof. Omi N and Associate Prof. Sagayama H proofread the text thoroughly. I am also grateful to Dr. Aoki K, Dr. Tokinoya K, and Dr. Sugasawa T for their detailed remarks. I would like to thank everyone at Takekoshi Laboratory for their help during my doctoral life. I would like to thank everyone who took part in this study. In addition, I would like to thank JST for the foundation. Finally, I also want to offer my appreciation to my family for their spiritual support and warm encouragement.

# X References


1. Solis-Herrera, C., et al., Pathogenesis of Type 2 Diabetes Mellitus, in Endotext, K.R. Feingold, et al., Editors. 2000, MDText.com, Inc.Copyright © 2000-2021, MDText.com, Inc.: South Dartmouth (MA).
2. Jin, Q. and R.C.W. Ma, Metabolomics in Diabetes and Diabetic Complications: Insights from Epidemiological Studies. Cells, 2021. 10(11).
3. Meyhöfer, S. and S.M. Schmid, [Diabetes complications - diabetes and the nervous system]. Dtsch Med Wochenschr, 2020. 145(22): p. 1599-1605.
4. Huebschmann, A.G., et al., Sex differences in the burden of type 2 diabetes and cardiovascular risk across the life course. Diabetologia, 2019. 62(10): p. 1761-1772.
5. Lake, A.J., A. Bo, and M. Hadjiconstantinou, Developing and Evaluating Behaviour Change Interventions for People with Younger-Onset Type 2 Diabetes: Lessons and Recommendations from Existing Programmes. Curr Diab Rep, 2021. 21(12): p. 59.
6. Andersson, C. and R.S. Vasan, Epidemiology of cardiovascular disease in young individuals. Nat Rev Cardiol, 2018. 15(4): p. 230-240.
7. Henning, R.J., Type-2 diabetes mellitus and cardiovascular disease. Future Cardiol, 2018. 14(6): p. 491-509.
8. Martín-Peláez, S., M. Fito, and O. Castaner, Mediterranean Diet Effects on Type 2 Diabetes Prevention, Disease Progression, and Related Mechanisms. A Review. Nutrients, 2020. 12(8).
9. Laakso, M., Biomarkers for type 2 diabetes. Mol Metab, 2019. 27s(Suppl): p. S139-s146.
10. Kanaley, J.A., et al., Exercise/Physical Activity in Individuals with Type 2 Diabetes: A Consensus Statement from the American College of Sports Medicine. Med Sci Sports Exerc, 2022. 54(2): p. 353-368.
11. Guess, N.D., Dietary Interventions for the Prevention of Type 2 Diabetes in High-Risk Groups: Current State of Evidence and Future Research Needs.

Nutrients, 2018. 10(9).

12. Vlachos, D., et al., Glycemic Index (GI) or Glycemic Load (GL) and Dietary Interventions for Optimizing Postprandial Hyperglycemia in Patients with T2 Diabetes: A Review. Nutrients, 2020. 12(6).
13. Salamone, D., A.A. Rivellese, and C. Vetrani, The relationship between gut microbiota, short-chain fatty acids and type 2 diabetes mellitus: the possible role of dietary fibre. Acta Diabetol, 2021. 58(9): p. 1131-1138.
14. Saji, N., et al., The Association between Cerebral Small Vessel Disease and the Gut Microbiome: A Cross-Sectional Analysis. J Stroke Cerebrovasc Dis, 2021. 30(3): p. 105568.
15. Arora, A., et al., Unravelling the involvement of gut microbiota in type 2 diabetes mellitus. Life Sci, 2021. 273: p. 119311.
16. Moszak, M., M. Szulińska, and P. Bogdański, You Are What You Eat-The Relationship between Diet, Microbiota, and Metabolic Disorders-A Review. Nutrients, 2020. 12(4).
17. Crovesy, L., T. El-Bacha, and E.L. Rosado, Modulation of the gut microbiota by probiotics and symbiotics is associated with changes in serum metabolite profile related to a decrease in inflammation and overall benefits to metabolic health: a double-blind randomized controlled clinical trial in women with obesity. Food Funct, 2021. 12(5): p. 2161-2170.
18. Yoon, H.S., et al., Akkermansia muciniphila secretes a glucagon-like peptide-1-inducing protein that improves glucose homeostasis and ameliorates metabolic disease in mice. Nat Microbiol, 2021. 6(5): p. 563-573.
19. Motiani, K.K., et al., Exercise Training Modulates Gut Microbiota Profile and Improves Endotoxemia. Med Sci Sports Exerc, 2020. 52(1): p. 94-104.
20. Aragón-Vela, J., et al., Impact of Exercise on Gut Microbiota in Obesity. Nutrients, 2021. 13(11).
21. Allen, J.M., et al., Exercise Alters Gut Microbiota Composition and Function in Lean and Obese Humans. Med Sci Sports Exerc, 2018. 50(4): p. 747-757.
22. Benson, A.K., et al., Individuality in gut microbiota composition is a complex

polygenic trait shaped by multiple environmental and host genetic factors. Proc Natl Acad Sci U S A, 2010. 107(44): p. 18933-8.

23. Xu, J., et al., Renalase is a novel, soluble monoamine oxidase that regulates cardiac function and blood pressure. J Clin Invest, 2005. 115(5): p. 1275-80.
24. Gao, Y., et al., Renalase is a novel tissue and serological biomarker in pancreatic ductal adenocarcinoma. PLoS One, 2021. 16(9): p. e0250539.
25. Guo, X., et al., Inhibition of renalase drives tumour rejection by promoting T cell activation. Eur J Cancer, 2022. 165: p. 81-96.
26. Wang, F., et al., Renalase might be associated with hypertension and insulin resistance in Type 2 diabetes. Ren Fail, 2014. 36(4): p. 552-6.
27. Buraczynska, M., et al., Renalase gene Glu37Asp polymorphism affects susceptibility to diabetic retinopathy in type 2 diabetes mellitus. Acta Diabetol, 2021. 58(12): p. 1595-1602.
28. Buse, J.B., et al., 2019 Update to: Management of Hyperglycemia in Type 2 Diabetes, 2018. A Consensus Report by the American Diabetes Association (ADA) and the European Association for the Study of Diabetes (EASD). Diabetes Care, 2020. 43(2): p. 487-493.
29. Taylor, S.I., Z.S. Yazdi, and A.L. Beitelshees, Pharmacological treatment of hyperglycemia in type 2 diabetes. J Clin Invest, 2021. 131(2).
30. Gandhi, G.Y. and A.D. Mooradian, Management of Hyperglycemia in Older Adults with Type 2 Diabetes. Drugs Aging, 2022. 39(1): p. 39-58.
31. Ceriello, A., et al., Glycaemic management in diabetes: old and new approaches. Lancet Diabetes Endocrinol, 2022. 10(1): p. 75-84.
32. Piché, M.E., A. Tchernof, and J.P. Després, Obesity Phenotypes, Diabetes, and Cardiovascular Diseases. Circ Res, 2020. 126(11): p. 1477-1500.
33. Greenwood, M., et al., Transcription factor Creb3l1 regulates the synthesis of prohormone convertase enzyme PC1/3 in endocrine cells. J Neuroendocrinol, 2020. 32(4): p. e12851.
34. Lafferty, R.A., et al., Proglucagon-Derived Peptides as Therapeutics. Front Endocrinol (Lausanne), 2021. 12: p. 689678.

35. Ramzy, A. and T.J. Kieffer, Altered islet prohormone processing: a cause or consequence of diabetes? Physiol Rev, 2022. 102(1): p. 155-208.
36. Saeedi, P., et al., Global and regional diabetes prevalence estimates for 2019 and projections for 2030 and 2045: Results from the International Diabetes Federation Diabetes Atlas, 9(th) edition. Diabetes Res Clin Pract, 2019. 157: p. 107843.
37. Okamura, T., et al., Ectopic fat obesity presents the greatest risk for incident type 2 diabetes: a population-based longitudinal study. Int J Obes (Lond), 2019. 43(1): p. 139-148.
38. Wu, H. and C.M. Ballantyne, Metabolic Inflammation and Insulin Resistance in Obesity. Circ Res, 2020. 126(11): p. 1549-1564.
39. Ahmed, B., R. Sultana, and M.W. Greene, Adipose tissue and insulin resistance in obese. Biomed Pharmacother, 2021. 137: p. 111315.
40. Zatterale, F., et al., Chronic Adipose Tissue Inflammation Linking Obesity to Insulin Resistance and Type 2 Diabetes. Front Physiol, 2019. 10: p. 1607.
41. Huang, X., et al., The PI3K/AKT pathway in obesity and type 2 diabetes. Int J Biol Sci, 2018. 14(11): p. 1483-1496.
42. Chen, Q., et al., JNK/PI3K/Akt signaling pathway is involved in myocardial ischemia/reperfusion injury in diabetic rats: effects of salvianolic acid A intervention. Am J Transl Res, 2016. 8(6): p. 2534-48.
43. Fatima, S.S., et al., Polymorphism of the renalase gene in gestational diabetes mellitus. Endocrine, 2017. 55(1): p. 124-129.
44. Teimoori, B., et al., Renalase rs10887800 polymorphism is associated with severe pre-eclampsia in southeast Iranian women. J Cell Biochem, 2019. 120(3): p. 3277-3285.
45. Zhang, F., et al., Association of renalase gene polymorphisms with the risk of hypertensive disorders of pregnancy in northeastern Han Chinese population. Gynecol Endocrinol, 2020. 36(11): p. 986-990.
46. Tokinoya, K., et al., Influence of acute exercise on renalase and its regulatory mechanism. Life Sci, 2018. 210: p. 235-242.

47. Tokinoya, K., et al., Gene expression level of renalase in the skeletal muscles is increased with high-intensity exercise training in mice on a high-fat diet. Physiol Int, 2021.
48. Tokinoya, K., et al., Moderate-intensity exercise increases renalase levels in the blood and skeletal muscle of rats. FEBS Open Bio, 2020. 10(6): p. 1005-1012.
49. Czarkowska-Paczek, B., et al., Exercise differentially regulates renalase expression in skeletal muscle and kidney. Tohoku J Exp Med, 2013. 231(4): p. 321-9.
50. Luo, M., et al., Aerobic Exercise Training Improves Renal Injury in Spontaneously Hypertensive Rats by Increasing Renalase Expression in Medulla. Front Cardiovasc Med, 2022. 9: p. 922705.
51. Aoki, K., et al., Renalase is localized to the small intestine crypt and expressed upon the activation of NF-κB p65 in mice model of fasting-induced oxidative stress. Life Sci, 2021. 267: p. 118904.
52. Pointer, T.C., F.S. Gorelick, and G.V. Desir, Renalase: A Multi-Functional Signaling Molecule with Roles in Gastrointestinal Disease. Cells, 2021. 10(8).
53. Czerwińska, K., R. Poręba, and P. Gać, Renalase-A new understanding of its enzymatic and non-enzymatic activity and its implications for future research. Clin Exp Pharmacol Physiol, 2022. 49(1): p. 3-9.
54. Mitsuoka, T., Intestinal flora and aging. Nutr Rev, 1992. 50(12): p. 438-46.
55. Ibal, J.C., et al., Review of the Current State of Freely Accessible Web Tools for the Analysis of 16S rRNA Sequencing of the Gut Microbiome. Int J Mol Sci, 2022. 23(18).
56. Gao, B., et al., An Introduction to Next Generation Sequencing Bioinformatic Analysis in Gut Microbiome Studies. Biomolecules, 2021. 11(4).
57. Abellan-Schneyder, I., et al., Primer, Pipelines, Parameters: Issues in 16S rRNA Gene Sequencing. mSphere, 2021. 6(1).
58. Korostin, D., et al., Comparative analysis of novel MGISEQ-2000 sequencing platform vs Illumina HiSeq 2500 for whole-genome sequencing. PLoS One, 2020. 15(3): p. e0230301.

59. Nguyen, N.P., et al., A perspective on 16S rRNA operational taxonomic unit clustering using sequence similarity. NPJ Biofilms Microbiomes, 2016. 2: p. 16004.
60. <ijs-44-4-846.pdf>.
61. Hall, M. and R.G. Beiko, 16S rRNA Gene Analysis with QIIME2. Methods Mol Biol, 2018. 1849: p. 113-129.
62. Poos, M.S., S.C. Walker, and D.A. Jackson, Functional-diversity indices can be driven by methodological choices and species richness. Ecology, 2009. 90(2): p. 341-7.
63. Ramette, A., Multivariate analyses in microbial ecology. FEMS Microbiol Ecol, 2007. 62(2): p. 142-60.
64. Mori, A.S., F. Isbell, and R. Seidl, β-Diversity, Community Assembly, and Ecosystem Functioning. Trends Ecol Evol, 2018. 33(7): p. 549-564.
65. Lozupone, C.A., et al., Quantitative and qualitative beta diversity measures lead to different insights into factors that structure microbial communities. Appl Environ Microbiol, 2007. 73(5): p. 1576-85.
66. Chang, F., S. He, and C. Dang, Assisted Selection of Biomarkers by Linear Discriminant Analysis Effect Size (LEfSe) in Microbiome Data. J Vis Exp, 2022(183).
67. Thingholm, L.B., et al., Obese Individuals with and without Type 2 Diabetes Show Different Gut Microbial Functional Capacity and Composition. Cell Host Microbe, 2019. 26(2): p. 252-264.e10.
68. Turnbaugh, P.J., et al., A core gut microbiome in obese and lean twins. Nature, 2009. 457(7228): p. 480-4.
69. Gurung, M., et al., Role of gut microbiota in type 2 diabetes pathophysiology. EBioMedicine, 2020. 51: p. 102590.
70. Han, J.L. and H.L. Lin, Intestinal microbiota and type 2 diabetes: from mechanism insights to therapeutic perspective. World J Gastroenterol, 2014. 20(47): p. 17737-45.
71. Qin, J., et al., A metagenome-wide association study of gut microbiota in type

2 diabetes. Nature, 2012. 490(7418): p. 55-60.

72. Zhao, J., et al., Dietary Fiber Increases Butyrate-Producing Bacteria and Improves the Growth Performance of Weaned Piglets. J Agric Food Chem, 2018. 66(30): p. 7995-8004.

73. Couto, M.R., et al., Microbiota-derived butyrate regulates intestinal inflammation: Focus on inflammatory bowel disease. Pharmacol Res, 2020. 159: p. 104947.

74. Mohammadi, S.O., et al., The impact of Helicobacter pylori infection on gut microbiota-endocrine system axis; modulation of metabolic hormone levels and energy homeostasis. J Diabetes Metab Disord, 2020. 19(2): p. 1855-1861.

75. Tanase, D.M., et al., Role of Gut Microbiota on Onset and Progression of Microvascular Complications of Type 2 Diabetes (T2DM). Nutrients, 2020. 12(12).

76. Wang, P.X., et al., Gut microbiota and metabolic syndrome. Chin Med J (Engl), 2020. 133(7): p. 808-816.

77. Everard, A., et al., Responses of gut microbiota and glucose and lipid metabolism to prebiotics in genetic obese and diet-induced leptin-resistant mice. Diabetes, 2011. 60(11): p. 2775-86.

78. Wang, Y., et al., Composite probiotics alleviate type 2 diabetes by regulating intestinal microbiota and inducing GLP-1 secretion in db/db mice. Biomed Pharmacother, 2020. 125: p. 109914.

79. Kaji, I., S. Karaki, and A. Kuwahara, Short-chain fatty acid receptor and its contribution to glucagon-like peptide-1 release. Digestion, 2014. 89(1): p. 31-6.

80. Tazoe, H., et al., Roles of short-chain fatty acids receptors, GPR41 and GPR43 on colonic functions. J Physiol Pharmacol, 2008. 59 Suppl 2: p. 251-62.

81. Benítez-Páez, A., et al., Sex, Food, and the Gut Microbiota: Disparate Response to Caloric Restriction Diet with Fiber Supplementation in Women and Men. Mol Nutr Food Res, 2021. 65(8): p. e2000996.

82. Barton, W., et al., The microbiome of professional athletes differs from that of more sedentary subjects in composition and particularly at the functional

metabolic level. Gut, 2018. 67(4): p. 625-633.

83. McCabe, L.R., et al., Exercise prevents high fat diet-induced bone loss, marrow adiposity and dysbiosis in male mice. Bone, 2019. 118: p. 20-31.

84. Aoki, T., et al., The Effect of Voluntary Exercise on Gut Microbiota in Partially Hydrolyzed Guar Gum Intake Mice under High-Fat Diet Feeding. Nutrients, 2020. 12(9).

85. Kulecka, M., et al., The composition and richness of the gut microbiota differentiate the top Polish endurance athletes from sedentary controls. Gut Microbes, 2020. 11(5): p. 1374-1384.

86. Lahiri, S., et al., The gut microbiota influences skeletal muscle mass and function in mice. Sci Transl Med, 2019. 11(502).

87. Domínguez-Balmaseda, D. and G. García-Pérez-de-Sevilla, The Relationship between the Gut Microbiota and Exercise: A Narrative Review. Hygiene, 2022. 2(4): p. 152-162.

88. Kumar, J., K. Rani, and C. Datt, Molecular link between dietary fibre, gut microbiota and health. Mol Biol Rep, 2020. 47(8): p. 6229-6237.

89. Wang, K., et al., Parabacteroides distasonis Alleviates Obesity and Metabolic Dysfunctions via Production of Succinate and Secondary Bile Acids. Cell Rep, 2019. 26(1): p. 222-235.e5.

90. Schoeler, M. and R. Caesar, Dietary lipids, gut microbiota and lipid metabolism. Rev Endocr Metab Disord, 2019. 20(4): p. 461-472.

91. Larsen, N., et al., Gut microbiota in human adults with type 2 diabetes differs from non-diabetic adults. PLoS One, 2010. 5(2): p. e9085.

92. Lê, K.A., et al., Alterations in fecal Lactobacillus and Bifidobacterium species in type 2 diabetic patients in Southern China population. Front Physiol, 2012. 3: p. 496.

93. Suzuki, T.A. and R.E. Ley, The role of the microbiota in human genetic adaptation. Science, 2020. 370(6521).

94. Goodrich, J.K., et al., The Relationship Between the Human Genome and Microbiome Comes into View. Annu Rev Genet, 2017. 51: p. 413-433.

95. Liu, X., et al., Metagenome-genome-wide association studies reveal human genetic impact on the oral microbiome. Cell Discov, 2021. 7(1): p. 117.
96. de Moura, E.D.M., et al., Diet-induced obesity in animal models: points to consider and influence on metabolic markers. Diabetol Metab Syndr, 2021. 13(1): p. 32.
97. Kleinert, M., et al., Animal models of obesity and diabetes mellitus. Nat Rev Endocrinol, 2018. 14(3): p. 140-162.
98. King, A.J., The use of animal models in diabetes research. Br J Pharmacol, 2012. 166(3): p. 877-94.
99. <56_263.pdf>.
100. Fraulob, J.C., et al., A Mouse Model of Metabolic Syndrome: Insulin Resistance, Fatty Liver and Non-Alcoholic Fatty Pancreas Disease (NAFPD) in C57BL/6 Mice Fed a High Fat Diet. J Clin Biochem Nutr, 2010. 46(3): p. 212-23.
101. Heydemann, A., An Overview of Murine High Fat Diet as a Model for Type 2 Diabetes Mellitus. J Diabetes Res, 2016. 2016: p. 2902351.
102. Kleinert, M., et al., Animal models of obesity and diabetes mellitus. Nat Rev Endocrinol, 2018. 14(3): p. 140-162.
103. Tokinoya, K., et al., Denervation-induced muscle atrophy suppression in renalase-deficient mice via increased protein synthesis. Physiol Rep, 2020. 8(15): p. e14475.
104. Tokinoya, K., et al., Effects of renalase deficiency on liver fibrosis markers in a nonalcoholic steatohepatitis mouse model. Mol Med Rep, 2021. 23(3).
105. Islam, M.R., et al., Weight Gain, Glucose Tolerance, and the Gut Microbiome of Male C57BL/6J Mice Housed on Corncob or Paper Bedding and Fed Normal or High-Fat Diet. J Am Assoc Lab Anim Sci, 2021. 60(4): p. 407-421.
106. Liang, H., et al., A high-fat diet and high-fat and high-cholesterol diet may affect glucose and lipid metabolism differentially through gut microbiota in mice. Exp Anim, 2021. 70(1): p. 73-83.
107. Chacko, E., Blunting post-meal glucose surges in people with diabetes. World J Diabetes, 2016. 7(11): p. 239-42.

108. Lin, X.J., H.F. Yang, and X.H. Wang, [Effects of aerobic exercise and dieting on chemerin and its receptor CMKLR1 in the livers of type 2 diabetic rats]. Zhongguo Ying Yong Sheng Li Xue Za Zhi, 2017. 33(5): p. 426-430.

109. McDonald, S.M., et al., The effects of aerobic exercise on markers of maternal metabolism during pregnancy. Birth Defects Res, 2021. 113(3): p. 227-237.

110. Zhou, Y., et al., Benefits of different combinations of aerobic and resistance exercise for improving plasma glucose and lipid metabolism and sleep quality among elderly patients with metabolic syndrome: a randomized controlled trial. Endocr J, 2022. 69(7): p. 819-830.

111. Emami, S.R., et al., Impact of eight weeks endurance training on biochemical parameters and obesity-induced oxidative stress in high fat diet-fed rats. J Exerc Nutrition Biochem, 2016. 20(1): p. 29-35.

112. Vogt É, L., et al., Metabolic and Molecular Subacute Effects of a Single Moderate-Intensity Exercise Bout, Performed in the Fasted State, in Obese Male Rats. Int J Environ Res Public Health, 2021. 18(14).

113. Beck, D. and J.A. Foster, Machine learning techniques accurately classify microbial communities by bacterial vaginosis characteristics. PLoS One, 2014. 9(2): p. e87830.

114. Yatsunenko, T., et al., Human gut microbiome viewed across age and geography. Nature, 2012. 486(7402): p. 222-7.

115. Kaul, A., O. Davidov, and S.D. Peddada, Structural zeros in high-dimensional data with applications to microbiome studies. Biostatistics, 2017. 18(3): p. 422-433.

116. Yu, D., et al., Profiling of gut microbial dysbiosis in adults with myeloid leukemia. FEBS Open Bio, 2021. 11(7): p. 2050-2059.

117. Liu, X., et al., A genome-wide association study for gut metagenome in Chinese adults illuminates complex diseases. Cell Discov, 2021. 7(1): p. 9.

118. Zhao, L., et al., A combination of quercetin and resveratrol reduces obesity in high-fat diet-fed rats by modulation of gut microbiota. Food Funct, 2017. 8(12): p. 4644-4656.

119. Lu, L., et al., Gut Microbiota and Serum Metabolic Signatures of High-Fat-Induced Bone Loss in Mice. Front Cell Infect Microbiol, 2021. 11: p. 788576.
120. Yang, B., et al., Lactobacillus reuteri FYNLJ109L1 Attenuating Metabolic Syndrome in Mice via Gut Microbiota Modulation and Alleviating Inflammation. Foods, 2021. 10(9).
121. Zhang, C., et al., Lactobacillus reuteri J1 prevents obesity by altering the gut microbiota and regulating bile acid metabolism in obese mice. Food Funct, 2022. 13(12): p. 6688-6701.
122. Xiao, Y., et al., Colonized Niche, Evolution and Function Signatures of Bifidobacterium pseudolongum within Bifidobacterial Genus. Foods, 2021. 10(10).
123. Lieber, A.D., et al., Loss of HDAC6 alters gut microbiota and worsens obesity. Faseb j, 2019. 33(1): p. 1098-1109.
124. Yuan, G., M. Tan, and X. Chen, Punicic acid ameliorates obesity and liver steatosis by regulating gut microbiota composition in mice. Food Funct, 2021. 12(17): p. 7897-7908.
125. Zhang, X., et al., Dietary cholesterol drives fatty liver-associated liver cancer by modulating gut microbiota and metabolites. Gut, 2021. 70(4): p. 761-774.
126. Hu, Y., et al., Pleurotus Ostreatus Ameliorates Obesity by Modulating the Gut Microbiota in Obese Mice Induced by High-Fat Diet. Nutrients, 2022. 14(9).
127. Singh, P., et al., High FODMAP diet causes barrier loss via lipopolysaccharide-mediated mast cell activation. JCI Insight, 2021. 6(22).
128. Meelu, P., et al., Impaired innate immune function associated with fecal supernatant from Crohn's disease patients: insights into potential pathogenic role of the microbiome. Inflamm Bowel Dis, 2014. 20(7): p. 1139-46.
129. Azaryan, A.V., T.J. Krieger, and V.Y. Hook, Purification and characteristics of the candidate prohormone processing proteases PC2 and PC1/3 from bovine adrenal medulla chromaffin granules. J Biol Chem, 1995. 270(14): p. 8201-8.
130. Magne, F., et al., The Firmicutes/Bacteroidetes Ratio: A Relevant Marker of Gut Dysbiosis in Obese Patients? Nutrients, 2020. 12(5).

131. Bo, T.B., et al., Bifidobacterium pseudolongum reduces triglycerides by modulating gut microbiota in mice fed high-fat food. J Steroid Biochem Mol Biol, 2020. 198: p. 105602.
132. Zhang, Q., et al., Influenza infection elicits an expansion of gut population of endogenous Bifidobacterium animalis which protects mice against infection. Genome Biol, 2020. 21(1): p. 99.
133. Zhang, H.Y., et al., Therapeutic mechanisms of traditional Chinese medicine to improve metabolic diseases via the gut microbiota. Biomed Pharmacother, 2021. 133: p. 110857.
134. Kaska, L., et al., Improved glucose metabolism following bariatric surgery is associated with increased circulating bile acid concentrations and remodeling of the gut microbiome. World J Gastroenterol, 2016. 22(39): p. 8698-8719.
135. Sun, L., et al., Ablation of gut microbiota alleviates obesity-induced hepatic steatosis and glucose intolerance by modulating bile acid metabolism in hamsters. Acta Pharm Sin B, 2019. 9(4): p. 702-710.
136. Tveter, K.M., et al., Polyphenol-induced improvements in glucose metabolism are associated with bile acid signaling to intestinal farnesoid X receptor. BMJ Open Diabetes Res Care, 2020. 8(1).
137. Spor, A., O. Koren, and R. Ley, Unravelling the effects of the environment and host genotype on the gut microbiome. Nat Rev Microbiol, 2011. 9(4): p. 279-90.
138. De Angelis, M., et al., The Food-gut Human Axis: The Effects of Diet on Gut Microbiota and Metabolome. Curr Med Chem, 2019. 26(19): p. 3567-3583.
139. Wang, H., et al., Phyllanthin inhibits MOLT-4 leukemic cancer cell growth and induces apoptosis through the inhibition of AKT and JNK signaling pathway. J Biochem Mol Toxicol, 2021. 35(6): p. 1-10.
140. Zheng, B., et al., Rhoifolin from Plumula Nelumbinis exhibits anti-cancer effects in pancreatic cancer via AKT/JNK signaling pathways. Sci Rep, 2022. 12(1): p. 5654.
141. Zhao, L., et al., MicroRNA-4268 inhibits cell proliferation via AKT/JNK

signalling pathways by targeting Rab6B in human gastric cancer. Cancer Gene Ther, 2020. 27(6): p. 461-472.

142. Wang, L., et al., Renalase prevents AKI independent of amine oxidase activity. J Am Soc Nephrol, 2014. 25(6): p. 1226-35.

143. Wu, Y., et al., Renalase improves pressure overload-induced heart failure in rats by regulating extracellular signal-regulated protein kinase 1/2 signaling. Hypertens Res, 2021. 44(5): p. 481-488.

144. Zhang, T., et al., Renalase Attenuates Mouse Fatty Liver Ischemia/Reperfusion Injury through Mitigating Oxidative Stress and Mitochondrial Damage via Activating SIRT1. Oxid Med Cell Longev, 2019. 2019: p. 7534285.

145. Razolli, D.S., et al., Proopiomelanocortin Processing in the Hypothalamus Is Directly Regulated by Saturated Fat: Implications for the Development of Obesity. Neuroendocrinology, 2020. 110(1-2): p. 92-104.

146. Tolhurst, G., et al., Short-chain fatty acids stimulate glucagon-like peptide-1 secretion via the G-protein-coupled receptor FFAR2. Diabetes, 2012. 61(2): p. 364-71.

147. Scott, K.P., et al., The influence of diet on the gut microbiota. Pharmacol Res, 2013. 69(1): p. 52-60.

148. Charrier, J.A., et al., High fat diet partially attenuates fermentation responses in rats fed resistant starch from high-amylose maize. Obesity (Silver Spring), 2013. 21(11): p. 2350-5.

149. Hoshino, A., et al., Modulation of PC1/3 activity by self-interaction and substrate binding. Endocrinology, 2011. 152(4): p. 1402-11.

150. Barnard, R.J., et al., Effects of a high-fat, sucrose diet on serum insulin and related atherosclerotic risk factors in rats. Atherosclerosis, 1993. 100(2): p. 229-36.

151. Barnard, R.J., et al., Diet-induced insulin resistance precedes other aspects of the metabolic syndrome. J Appl Physiol (1985), 1998. 84(4): p. 1311-5.

152. Bilu, C., et al., Beneficial effects of voluntary wheel running on activity rhythms, metabolic state, and affect in a diurnal model of circadian disruption. Sci Rep,

2022. 12(1): p. 2434.

153. Tanaka, Y., et al., Effect of a single bout of morning or afternoon exercise on glucose fluctuation in young healthy men. Physiol Rep, 2021. 9(7): p. e14784.

154. Wang, H., et al., Effects of Different Intensity Exercise on Glucose Metabolism and Hepatic IRS/PI3K/AKT Pathway in SD Rats Exposed with TCDD. Int J Environ Res Public Health, 2021. 18(24).

155. Lee, S., et al., Effects of long-term exercise on plasma adipokine levels and inflammation-related gene expression in subcutaneous adipose tissue in sedentary dysglycaemic, overweight men and sedentary normoglycaemic men of healthy weight. Diabetologia, 2019. 62(6): p. 1048-1064.

156. Younossi, Z.M., K.E. Corey, and J.K. Lim, AGA Clinical Practice Update on Lifestyle Modification Using Diet and Exercise to Achieve Weight Loss in the Management of Nonalcoholic Fatty Liver Disease: Expert Review. Gastroenterology, 2021. 160(3): p. 912-918.

157. Ahmed, S. and J.D. Spence, Sex differences in the intestinal microbiome: interactions with risk factors for atherosclerosis and cardiovascular disease. Biol Sex Differ, 2021. 12(1): p. 35.